POLITECNICO DI TORINO

Master's degree in Mechatronic Engineering

Master's degree thesis

Development and experimental testing of a control strategy for adaptive assistance delivered by a semi-passive upper-limb exoskeleton

Supervisors

Prof. Marcello Chiaberge
Dr. Simona Crea
Prof. Nicola Vitiello

Tutors

Dr. Lorenzo Grazi
Dr. Emilio Trigili

Candidate

Giulia Ramella

Academic Year 2020/2021
Discussion session - October 2021

ABSTRACT

Work-related musculoskeletal disorders (WMSDs) are one of the most common causes of occupational disease in Europe. They typically cause muscle fatigue and injuries, leading to a relatively high number of lost workdays with a negative impact on enterprises' productivity and the increased burden on national healthcare systems, as reported by the EU-OSHA in 2007.

In recent years, in order to reduce workers' fatigue and the insurgence of WMSDs, a growing interest in wearable robotics (WR) technologies has led to the application of upper-limb exoskeletons for industrial applications. The state of the art provides many examples of passive devices where the assistive action (e.g. assistive torque) is generally achieved by means of passive mechanisms, like springs and dampers.

Despite their light weight and potentialities in reducing workers' muscular strain, they still have the intrinsic lack of adaptivity to different tasks (e.g. static or dynamic) or different physiological state of their users (e.g. increased fatigue). Indeed, once the support level is selected at the beginning of the work it remains fixed at a certain level for the whole duration of the task, unless the worker manually adjusts it.

At the leading edge of this research field, the WR Laboratory of Scuola Superiore Sant'Anna of Pisa is currently investigating innovative solutions. This thesis, developed within the WR Laboratory, aims at designing, developing, and eventually implementing an adaptive algorithm for the automatic selection of the support level for a semi-passive upper-limb exoskeleton (H-PULSE). The exoskeleton was developed by IUVO S.r.l., a spin-off company of Scuola Superiore Sant'Anna, within the H2020 HUMAN project (Grant Agreement n. 723737, website: http://humanmanufacturing.eu). The H-PULSE is embedded with sensors, to monitor the shoulder flexion/extension angle, and an active tuning mechanism that allows to automatically change, in real time, the pre-tensioning of the springs responsible for the assistive torque peak.

The algorithm developed in this work of thesis exploits shoulder kinematics to compute movement-related features to online estimate the desired level of support. In particular, the movements features are linearly combined in a finite different equation formulation to compute the level of assistance that the exoskeleton needs to provide. The algorithm was first designed and simulated offline in MATLAB R2019b and then translated in LabView 2018 for evaluating its real-time performance. Finally, the algorithm was implemented in the real-time processor of the H-PULSE exoskeleton for experimental testing.

The algorithm was evaluated with human-in-the-loop experimental trials, with the main objectives of investigating the effects of the adaptive control strategy against experimental conditions where the exoskeleton was not worn (i.e. without any support) or delivered a fixed and predetermined level of assistance (i.e. supporting about the 50% of the arm gravitational torque).

Special thanks to my whole family, for their guidance and continuous support;
to all my friends, for their encouragement and everyday entertainment; and
to my thesis supervisors, for their mentoring and inspiring advice.

TABLE OF CONTENTS

LIST OF FIGURES

LIST OF TABLES

1 INTRODUCTION

1.1 MOTIVATIONS: WORK RELATED MUSCULOSKELETAL DISORDERS

According to the European Agency for Safety and Health at Work (EU-OSHA), work related musculoskeletal disorders (WMSD) identify all the impairments of body structures as muscles, joints, tendons, ligaments, nerves, bones and circulation system that are related and caused by work and by the environment in which a certain task is performed [1].

These disorders are increasing in work environments and, according to a recent study, they affect three out of five workers in the EU [2]. The impact of these conditions has been evaluated by the EU-OSHA and it can be seen how WMSDs affect the single workers as well as the society as a whole, highlighting how much this problem represents a multi-sectoral issue. It is difficult to have unique metrics to assess how these conditions affect the European industries and workers. However, multiple studies emphasized how WMSDs can directly affect the industries' economy and the worker's health.

First of all, WMSDs are responsible for longer absences from work. An important example resides in an Austrian study that highlighted how the 24.3% of the lost working time was related to this kind of disease. The same study found that WMSDs were responsible for a quarter of the long absences from work (more than 6 weeks), that were the 35% of the overall lost workdays [3]. Another significant impact of WMSDs is on the economic costs, since productivity losses due to occupational illnesses can be significant. As an example, in Germany it was estimated that musculoskeletal and connective tissue disorders constituted a 17.2 billion in production loss based on labour costs in 2016 [2]. Moreover, the healthcare point of view must be considered. WMSD require the investment of time and financial resources to provide rehabilitation to the patient and reintegrate workers that have suffered from these conditions [1]. Even if the condition is resolved, the workers may still have to deal with long-term effects of WMSDs, since these disorders cause overall fatigue, sleeping problems and anxiety, thus heavily affecting the mental health of individuals [2]. To quantify the gravity of the WMSDs consequences on the workers' well-being, an important metric is the disability-adjusted life years indicator, indicating the years lost as a result of an illness. It was estimated that these disorders are responsible for 15% of the total number of years lost related to work injuries and illnesses [2].

Despite all these negative consequences related to WMSDs, it is not straight-forward to take actions to contrast the insurgence of these diseases. This difficulty resides in the fact that the main causes behind the insurgence of WMSDs can be related, among others, to working conditions with demanding force applications (pulling, pushing, tools usage), repetitive movements, awkward prolonged body postures, repetitive and monotonous tasks [1]. All these conditions are usually unavoidable in most of the industry tasks.

A possible solution to avoid demanding movements is to fully automatize the work environment. This drastic measure would imply the removal of the human worker in favour of a fully robotized environment. However, this decision implies some ethical and organizational problems. A study remarked the limitations of this measure: first of all, it would imply high costs. Secondly, the manipulators have limited versatility and adaptability, whereas human cognitive skills and flexibility still have a crucial role in most of the working conditions [4].

All these premises lead to the need to take serious actions to preserve the workers' health and industry economy. The variability of factors that lead to WMSDs make it difficult to identify the best strategy to contrast the insurgence of these diseases. A first suggestion is to have an early intervention, which is crucial to minimize the impact of WMSD on the workers and more generally on the enterprises. Moreover, the European Survey of Enterprises suggests to use an integrated approach to this problem, considering that single measures have been demonstrated to be less constructive than integrated ones [2]. The prevention approach becomes crucial in the contrast to the insurgence of WMSDs. The reports from the European Agency for Safety and Health at Work have concluded that the risk assessment and prevention approach can be successfully applied to the prevention of WMSD [3]. A particular focus is put on the key factors to consider when applying prevention measures. First of all, facing the many risk factors, a holistic approach is suggested, considering the demanded load on the body as well as the work organization. At the same time, the diversity of the population implies an inclusive approach to consider each worker's needs and capabilities.

Moreover, body postures have a central role and it is crucial to consider the need to vary the working postures to avoid the maintenance of same positions for prolonged time. This preventive measure becomes more important in case of repetitive and monotonous jobs, where it is paramount to provide a sufficient degree of variety in order to have an effective prevention measure.

This integrated approach that takes into account the interaction between the worker and the work environment is gaining more importance in recent years. One of the reasons behind this trend resides in the introduction of the concept of Industry 4.0 worker. This term denotes a worker that understands and cooperates in its work environment by means of a smart interaction with the machines and the robots [5]. The central topic of Industry 4.0 is indeed a so-called human-centric manufacturing, where the aim is to fully exploit the potential of both the operator and the industry to have a socially sustainable manufacturing industry.

1.2 FOCUS ON SHOULDERS AND THEIR TASKS

In the field of work-related disorders, a particular focus must be made on shoulder related illnesses: as observed by the European Agency for Safety and Health at Work, shoulder and neck pains are reported by 23% of the workers [3]. The US Department of Health and Human Services made a critical review on these work-related disorders, with a chapter dedicated to shoulder problems [6]. The authors highlighted the associations between shoulder WMSDs and certain types of work with important evidence-based conclusions. In order to fully understand shoulder WMSDs, it is worth making a small overview of the shoulder complex under the anatomy and physiology point of view.

1.2.1 Shoulder joint

The shoulder joint, also known as glenohumeral joint, is one of the most complex articulation of the human body, roughly described as a ball and socket joint [7]. It allows the largest range of motion in the human body and connects the upper limbs to the trunk. The main bones of the joints are the clavicle, the scapula and the humerus (Figure 1). The first is positioned above the first rib and is directly connected to the scapula. The scapula is a flab bone with many muscular attachments and it is connected to the humerus via the glenohumeral joint [7]. Even if many muscles are responsible for the stability and movement of this joint, the main muscles that support the shoulder are the ones belonging to the rotator cuff [7]. This muscle group is composed of the supraspinatus, infraspinatus, teres minor and subscapularis and it has a crucial role in the support of the shoulder.

Among the muscles that are worth mentioning, the trapezius, located in the back, is the one responsible for the lowering of the shoulder (assisted by gravity in the upright position). Always located in the posterior part, the latissimus dorsi is a large muscle in the middle of the back. Moving into the frontal part, the pectoralis is large muscle responsible for the rotation of the arm and the breathing action. Another important muscle is the deltoid: it is located more superficially on the side of the shoulder and it is fundamental for the movements of the humerus. The deltoid is composed of three origins, each of them responsible for a precise movement: the anterior deltoid flexes the humerus, the middle abducts it and the posterior rotates it. Considering the muscles located in the arms, the two main antagonists' muscles are represented by the biceps and the triceps. The former is located in the front of the arm, it is composed of two heads and it connects the shoulder to the elbow. The latter is located in the back of the arm and spans from the shoulder to the elbow.

Overall, the shoulder muscles are fundamental for both the motion and the stability of the joint [7]. In particular, this complex joint allows for a wide range of motion, allowing the movement of adduction/abduction, flexion/extension and intra/extra rotation. In order to meet both the requirements on mobility and stability, the shoulder complex has to perform a dynamic stabilization

[8]. Through active forces, the dynamic stability is achieved by means of both passive forces (from ligaments and articular surface) and from active forces (relying on muscles). However, it is not straight forward to meet the stability and mobility needs, therefore the shoulder complex is highly susceptible to disorders and instability.

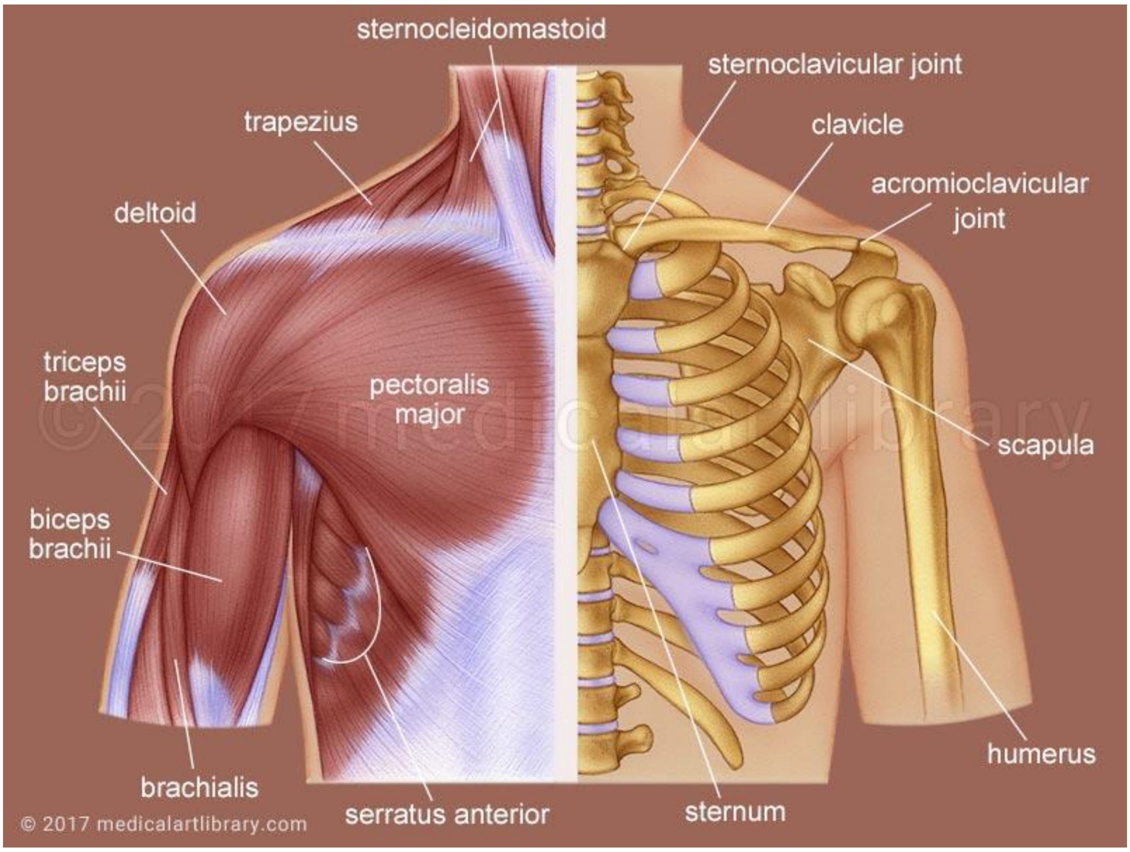

Figure 1: Shoulder anatomy – muscles and bones by Lauren Keswick. Downloaded with permission from MedicalArtLibrary [9].

1.2.2 Shoulder tasks and WMSDs

The relationship between WMSDs and shoulder tasks has been widely studied. It is worth citing the report of the European Agency for Safety and Health at Work [6]. In this paper, the authors gathered evidence of the relationship between shoulder pains and the work factors that may be behind the insurgence of these diseases. They identified precise movements as critical for the shoulder articulation, identifying awkward postures as one of the most demanding condition. The neutral body posture implies the arms elongated along the body, whereas awkward postures may occur when the arms are moved in unusual positions, often aggravated by prolonged or repetitive movements.

Another critical condition can be found when forceful exertions are required, meaning that the shoulder has to carry or move heavy loads or tools. Lastly, another demanding movement is represented by repetitive exertions, that indicate movements repeated in a similar fashion for many times within a certain cycle.

In order to clarify where these problems may occur in jobs, some studies can be taken as an example. For what concerns non-ergonomic movements, a study conducted on workers performing jobs on industrial assembly lines highlighted how the static tasks involved were linked to shoulder tendinitis [10]. The same study also pointed out the direct association of shoulder disorders to the percentage of time spent with the arms elevated or abducted (with an angle greater than 60 degrees) [10].

Another study was conducted on construction workers exposed to load lifting. This research showed how there was a direct relation between acromioclavicular osteoarthrosis and the required shoulder movements [11]. Moreover, a cross sectional study on 1886 males from 3 different occupational groups (machinists, mechanics and painters) established the quantitative relations between the works implying repetitive and elevated arms postures and clinically confirmed shoulder issues [12]. In particular, upper arm elevations above 90 degrees were associated with supraspinatus tendinitis and shoulder pain.

1.3 Solutions to prevent shoulder WMSDs

Prevention of WMSDs is a challenge that the EU is facing by providing detailed regulations to successfully integrate the workers' participation and the work adaptation to the individual. The main goal of these measures is to improve the safety and health of workers, according to the principle of "participatory ergonomics" [13]. This expression defines the "involvement of people in planning and controlling a significant amount of their own work activities, with sufficient knowledge and power to influence both processes and outcomes to achieve desirable goals" [14]. The importance of this concept resides in the fact that participatory ergonomics programs can successfully reduce the incidence of WMSD [15].

The workers central role in the workspace ergonomics is a concept that is expressed also in the Operator 4.0, a key idea for Industry 4.0. This term denotes a worker with the ability to understand and interact with the machines in a smart way in order to create a trusting work environment that can enhance the operator skills and abilities [5].

A significant example of the application of this principle can be seen in the building strategy for a new plant that Volvo opened for the assembling of cars in Sweden. The aim of the design was to improve the work productivity and quality along with the ergonomic conditions and the work organization [16]. The plant implemented a tilting device that rotated and lowered the car body to facilitate assembly work, resulting in the main effect of enhancing the job ergonomics without compromising the productivity [16].

Although solutions like the one implemented by Volvo and other car manufacturers seem very promising, it is not always possible to adopt these measures in a production plant: a relevant limitation of the cited study was that the plant was built from scratch. In many other cases, industrial applications already have existing structures and modifications could imply heavy changes in the manufacturing process and expensive investments [17].

Another proposed solution to help workers in physically demanding and non-ergonomic work activities is to integrate robotic manipulators in the work environment. However, even if automation is growing in many fields, several tasks cannot be fully automated since the associated costs would be too high and human cognitive abilities and flexibility still outperform the ones of robots [4]. Therefore, the workers role is central and in recent years a new solution has been proposed to be integrated in the work environment: wearable robots.

1.4 WEARABLE ROBOTICS FOR INDUSTRIAL APPLICATION

Wearable robots (WR) are mechatronic systems designed to assist human motion exploiting mechatronic devices attached to the human body [18]. One of the first intended use of WR is for rehabilitation, where fixed robotic stations are used to provide rehabilitation exercise. The benefits of rehabilitation WR are multiple over conventional methods: it is less dependent on clinical staff availability, it delivers precise forces applied depending on the level of recovery needed and it can deliver repetitive actions at a reasonable cost [19]. The WR are widely studied also in the military field, where their potential to augment the strength and endurance of humans is exploited to reach rugged environments [20]. In recent years, a further exploitation of WR is for devices to assist industry workers. Specifically, WR are designed to provide assistance in particular tasks that require awkward postures and repetitive movements which, as said above, are among the main causes of WMSDs insurgence. The intent of these exoskeletons is to enhance and help the humans is particularly demanding movements by means of an external wearable structure. The augmentation of human capabilities is a central idea of the Operator 4.0, where exoskeletons represent a perfect example of trade-off between automation and manual tasks [5].

The main challenge in the design of assistive WR is to successfully integrate the human body with the mechatronic WR system. This task is not straight-forward since the human body is a complex kinematic structure which is difficult to replicate and follow with a mechatronic structure [18]. The actions between the robot and the human must be coordinated, therefore the human body has a central role in the design of a WR device [21]. As a consequence, the interface with a robot must fulfil some specific requirements.

First of all, the system must guarantee the safety of the user, thus not constraining to strange or unnatural movements that could harm the human joints [21]. Moreover, the comfort is crucial for a wearable device, since it should adapt to the ergonomics of the human and not cause any unwanted pressure on the body [21]. The human joints must be aligned with the robot ones otherwise undesired forces may be generated and impede movements. Additionally, the WR operational space has to be compatible with the natural movements allowed by the user [21].

Since the main goal of a WR is to deliver specific forces to help the user in some specific motions, the design must carefully consider the intensity and the way in which those forces are delivered. The force transmission is done through the so called pHRI, the physical human-robot interface. In the case in which the pHRI integrates a control system, it must guarantee the full and safe cooperation of the human motions and the WR motor control [21]. Moreover , the device must be easily donned on and off, therefore guaranteeing an intuitive way of wearing it for a trained user [22].

Furthermore, there should be no need of tools to regulate the device, which also has to be adjustable to fit a large percentage of the population [22]. A last crucial point is the user acceptability, fundamental for the correct use and acceptance of the device. It has been underlined that a familiarization phase is paramount in order to have a faster understanding and acceptance from the workers and thus a quicker adoption in industries [23].

Moving into biomechanical aspects, the mechanical requirements for a WR must be followed carefully. It has to be remarked that if the device movements are not following the human motion, some discomfort may arise. In more technical terms, kinematic incompatibility between WR and limbs occur. This can be caused by wrong designs but also arise from the variability of the human biomechanical parameters during motion or between different subject [21].

Firstly, for what concerns inter-subject variability, estimation of the anatomical measures can be difficult since each individual has its own measurements. For this issue, it is crucial to make the devices adaptable and easy to regulate around someone's shape. Additionally, a necessity for a familiarization protocol to ease the donning/doffing and regulation of the devices is important for a correct knowledge of the device [23]. Secondly, one of the main difficulties in the design of WR is taking into account the variability of the axes alignments and location, since the instantaneous centres of rotation are subject to motions during movements [21].

Generally speaking, if kinematic requirements are not met, incompatibilities may lead to kinematic misalignments. Macro misalignments happen if joints interactions between the device and the human joint are overly simplified, thus the necessity to carefully chose the kinematic chain to have the correct number of degrees of freedom [21]. Another problem is represented by micro misalignments, which are always caused by non-coinciding axes but, in this case, cannot be avoided. In fact, they are caused by the difficulty to perfectly follow the human movements with a WR and the impossibility to exactly know the position of the instantaneous centres of rotation during motion [21].

1.4.1 WR for upper limbs

One of the main applications of WR is for upper limb devices for industry, helping to relieve the shoulder from fatiguing tasks. The main intent of these devices is to provide a torque to the user so that the gravity action on the arm is compensated [24]. The exoskeletons efficacy to reduce the physical strain in demanding shoulder tasks has been assessed by many studies over the years [4], [23]–[29]. These efficacy assessments directly imply the potential of wearable devices to reduce the risk of WMSDs insurgence [25]. As a consequence of the promising results obtained with commercially available devices, many industries around the world have already adopted these devices in their working environments. A notable example includes a Toyota plant in Canada where WR devices are used for undercarriage assembly [30]. From the Wearable Robotics Association Conference (WearRAcon19) held in March 2019 it emerged that other global leaders such as BMW, Ford, Honda, Nissan, Toyota, and Volkswagen are currently exploiting WR devices [31].

For the design of an upper limb device, a complete knowledge of the arm kinematics is necessary. In the literature, complete models of the arms have been derived from specific tables [32] and described by means of the Denavit-Hartenberg (D-H) convention (Figure 2). When considering the full model, the most common description is by means of a 7 DOFs (degrees of freedom) model, where the shoulder comprises 3 DOFs, the elbow and the wrist account for 2DOFs each [21], [33].

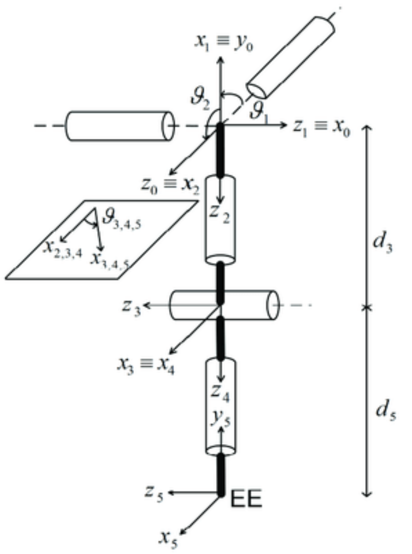

ϑ	d	a	α
$\vartheta_1 + \pi/2$	0	0	$\pi/2$
$\vartheta_2 + \pi/2$	0	0	$-\pi/2$
ϑ_3	d_3	0	$-\pi/2$
ϑ_4	0	0	$\pi/2$
ϑ_5	d_5	0	$-\pi/2$

Figure 2: Denavit-Hartenberg convention for the description of the human arm [33].

Although the D-H convention provides a detailed mathematical description, a simplified approach can be used to have a general idea of the forces acting on the shoulder. Since most of the WR for upper limbs focus on the flexion/extension movement, it is worth reporting the simplified force scheme used for the design of a supportive mechanism to assist the arm elevation. The force diagram reported in Figure 3 shows the forces and the corresponding levers that globally generate the torques acting on the arm [22]. The gravity force acting on the arm (denoted as G) has to be compensated by the muscles force (F_M), thus needing the help of additional support (F_s and F_r) provided by the wearable device.

Moreover, the gravity acting on the arm that has to be compensated by the WR action has a force profile that has a parabolic shape depending on the angle of elevation considered, as shown in Figure 3. As a consequence, the assistive torque profile provided by the exoskeleton has to match the biological gravitational angle-torque to effectively reduce the load on the upper limbs [27].

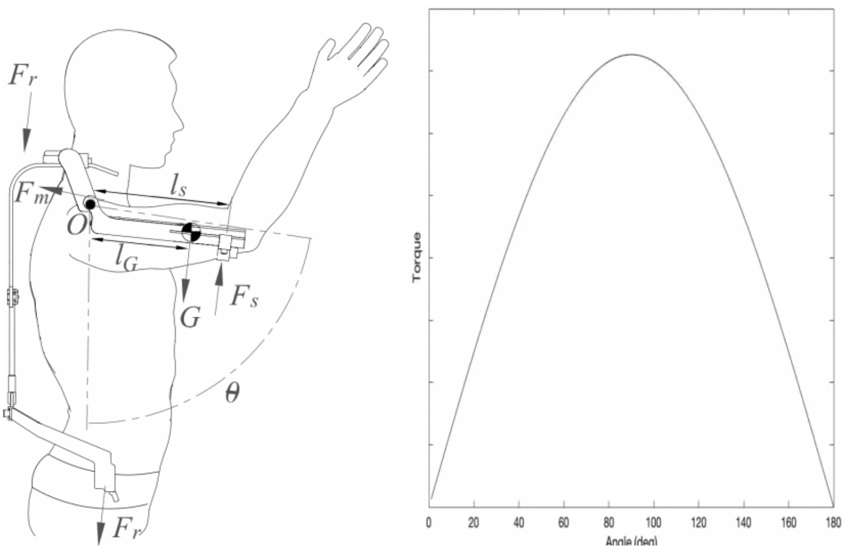

Figure 3: Forces diagram and gravity torque profile acting on the arm during flexion-extension [24] *© 2019 IEEE.*

As a last point concerning WR for upper limbs, the most important classification can be done by considering the type of mechatronic system adopted in the design. The distinction is made between passive and active devices. First of all, passive WR devices are not powered and exploit only passive mechanical systems. By means of springs/dampers they can store the energy and deliver it when needed for specific movements [4]. Additionally, they transfer the forces to other parts of the body, for instance from the shoulders to the pelvic area [4]. Moreover, they do not require power nor control electronics [34], which implies lighter and safer solutions [4]. On the other hand, active devices include actuators to augment the human power and to help in the joints movements [25]. Among electromechanical, hydraulic and pneumatic actuators, the electrical ones are the most used for active solutions for their high controllability and precision [35].

The design of this type of devices must follow strict requirements on the safety and health of the end-user. Nowadays, the commercially available devices are mostly passive, such as EksoVest (EksoBionics, Richmond, California), Airframe (Levitate Technologies, San Diego, California), ShoulderX (SuitX Emeryville, California), PAEXO (Ottobock, Duderstadt, Germany), and SkelEx (SkelEx, Rotterdam, The Netherlands).

The reason behind the large diffusion of passive devices relies in some intrinsic limitations of active exoskeletons. In fact, active devices imply a more complicated safety assessment following the difficulty to have a correct intention detection to give support to the user only when it is actually needed [34]. Moreover, an important downside of active solutions if the resulting structure that can be too bulky and heavy for the end user [36]. On the other hand, passive devices have a hard-coded mechanical structure to provide the desired support. This solution makes the devices lighter, more manageable, without control-related issues and intrinsically safer and easier for the end-user [26].

In this general framework, an innovative approach is to explore a semi-passive device. The main intent of this new solution is to implement a smarter and more adaptive device while keeping the light and compact design. This thesis work exploits indeed a semi-passive exoskeleton, the H-PULSE, to provide a bioinspired assistance to the shoulders [36]. This device presents two innovative features: an active tuning mechanism to regulate the pre-tensioning of the springs and integrated angle sensors to measure shoulder movements. In order to make the device adaptable to the user movements, this thesis develops an adaptive algorithm to change in real time the delivered assistance. From kinematic features computed from the sensors data, the desired assistance is selected and changed in real-time by modifying the pre-tensioning of the springs. The algorithm efficacy is validated in experimental trials with a human-in-the-loop testing.

1.5 Objective of the thesis

In the field of wearable robotics for upper-limbs, the promising results with commercially available devices lead the way for the research of new solutions. Starting from passive devices, there is the increasing need to design more advanced exoskeletons, while maintaining the safety and intuitiveness of existing devices. The main limitation of passive WR resides in the impossibility to change the desired level of assistance once it has been set. Facing the variety of industry tasks, that are usually diversified and less structured, it has been suggested that an on-line adaptation of the level of support could be a new line of research [4].

To the best of the author’s knowledge, there is no current device that implements such adaptivity feature. Some solutions tried to implement regulations to change the assistance while the device is worn. Most notably, the SkelEx exoskeleton presents three buttons that allow to adjust the peak torque and assistive torque profile depending on the user needs and performed activity [24]. However, the manual selection of the support is still required in this solution, since no automatic change is implemented. Another study explored the possibility to implement a button on the user glove to allow the worker to increase or decrease the support while working. This solution is straight-forward and is promising to increase the user acceptance by giving the feeling of control over the device [37]. Although encouraging, the need to introduce a glove may not be optimal for most industry tasks and implies the risk to reduce dexterity. A clever strategy could be implemented starting from kinematics information on the user movements. Indeed, this path has been explored in the design of the Stuttgart Exo-Jacket, an active exoskeleton where the control loop takes as inputs the muscles activations and the arms movements [35].

Taking inspiration from these results, this thesis aims at developing an adaptive algorithm based on arms kinematics that can automatically change the support level of the semi-passive exoskeleton H-PULSE. Kinematics data are extracted from the exoskeleton angle sensors and used to compute the desired assistance. The algorithm is conceived to be task independent and possesses the ability to describe the system history be means of a finite difference equation formulation. In order to assess the algorithm efficacy, a human-in-the-loop validating procedure is implemented.

1.6 OUTLINE OF THE THESIS

This thesis work is structured as follows. Chapter 2 covers the main existing solutions for both active and passive devices, as well as the main design choices for each wearable robot. In Chapter 3 the semi-passive exoskeleton H-PULSE is described in details, with subsections dedicated to the mechatronics and control strategies of the device. Chapter 4 presents a full description of the adaptive algorithm, with additional sub-chapters dedicated to the offline implementation and simulation. In Chapter 5 the experimental activities are presented, with an exhaustive presentation of the human-in-the-loop procedure and the metrics for the efficacy assessment. Finally, Chapter 6 discusses the obtained results and Chapter 7 represents the final conclusions of the thesis work.

2 STATE OF THE ART ON EXISTING SOLUTIONS

In this chapter, the main existing solutions related to upper-limb exoskeletons are briefly presented. The state of the art presents a wide range of examples and, in order to have a clear presentation, these chapters follow the typical classification used for exoskeletons. Indeed, depending on the type of actuation, devices can be passive or active.

2.1 PASSIVE SOLUTIONS

2.1.1 PAEXO

The PAEXO (Ottobock, Duderstadt, Germany) device is a passive upper-limb exoskeleton developed by the German industry Ottobock, a worldwide leader in prosthetics (Figure 4). This exoskeleton is designed to provide maximum freedom of movement and comfort to the user with a reasonable level of assistance [4].

This solution is designed to transfer the arms weight to the pelvis, where it is supported by a hip belt. The assistive part is composed of a support bar, where the necessary torque is generated through a passive actuator based on a spring mechanism. In the lower part of the support bar, a cable mechanism transfers the supportive action to the arms. In fact, the cable is connected at one end to the spring, whereas the other goes to the end of the arm bar. This arm bar is connected to the upper arm bracelets through a hinge joint.

The amount of support provided depends on the resulting lever length of the arm bar with respect to its passive joint. The support can therefore easily be manually tuned, making it adaptable to the user arm weight or to the extra tool mass to be supported. The supportive torque profile has a peak at around 90 degrees of arm elevation, whereas it decreases to zero when the arms are resting along the body [29]. A stabilizing structure (straps attached to the hip belt) keeps the device close to the body, without compromising the shoulder movements [4].

Overall, the device is lightweight (1,9 kg) and allows freedom of movements of the trunk and of the upper limbs, proving supportive torque when overhead tasks are performed. Moreover, the device can be adjusted in the hip belt, arm brace and support bar, in order to be adapted to different users' anthropometries.

Several studies have been carried out to assess the efficacy of this device. A first study found a reduction in the heart rate and in the muscles activations when using the exoskeleton, concluding that the use of this device could reduce the shoulder WMSD [29]. Another research highlighted how the device did not reduce the range of the human movements, while being helpful during overhead work to reduce users' physical strain [4].

Figure 4: Paexo exoskeleton by Ottobock [4] *© 2020 IEEE.*

2.1.2 Levitate Airframe

The Levitate Airframe is an exoskeleton developed by Levitate Technologies (Figure 5). This device is intended to support workers that perform repetitive arm movements and static elevations [26].

The design aims at transferring the weight of the arms from the shoulder and neck to the core of the body, thanks to the presence of passive elements along the arms. A metallic frame is designed to fit the user body and allows unconstrained movements. The mechanical passive elements are located along the arms and provide support to the arm through arm sets.

The support is not active when the arms are elongated along the body, whereas it increases when the arms are raised. The amount of support given and the angles at which this contribution is delivered can be manually tuned. More specifically, the exoskeleton has different sets of mechanical passive elements so that the user can choose the desired level of assistance depending on the task and weight (if a tool is used) that has to be supported.

The device weighs 2.3 kg and is easy to be worn by the worker. Moreover, it can be custom fit in the size of the arm-sets, shoulder and waist straps. This characteristic is fundamental for the user comfort, providing freedom of movements without limiting the workspace.

In recent years, some studies analysed the efficacy of this exoskeleton. One study assessed the efficacy of the device when used for static and dynamic tasks [26]. The results highlighted an increased performance and less fatigue perception when working with the exoskeleton. A second study assessed the benefits of the exoskeleton in terms of fatigue and muscles activations in short terms real work conditions [30].

Figure 5: Levitate Airframe exoskeleton by Levitate Technologies [26].

2.1.3 ShoulderX

The ShoulderX (SuitX, Emeryville, CA, USA) has been developed by the Human Engineering Laboratory of the University of California with the intent of supporting the arms during repetitive and overhead tasks [24].

The design of this exoskeleton is intended to provide the arm with a supportive torque so that the action usually performed by the muscles to counteract gravity is relieved. A frame connects the user to the device, aiming also at redistributing the weights from the upper arms to the hips (Figure 7). An actuator at the shoulder joint level generates the required supportive torque. The workspace of the arms is not limited thanks to the 2 degrees of freedom in the spine and 3 in the shoulder [22].

The latest version of the device includes indicators for all settings [24]. This device is designed with some peculiar features with respect to the main competitors (Figure 6). First of all, an asymmetric torque profile is used to have a zero-torque range where no support is desired, thus at very low or very high angles. The zero-torque area is modifiable to some extent, since the main intention is to keep the curve similar to the natural gravity profile. This approach optimizes the support when primary work-related overhead tasks are executed, while during secondary movements it avoids.

Another adjustment can change the peak torque position with respect to the angle of elevation and the level of support. This latter tuning allows to change the amount of torque that the device can deliver and it can be tuned by manually regulating the spring-cable system present in the actuator. Lastly, the stiffness of the device can easily be regulated thanks to a coupling of two parallel-concentrically springs and the corresponding switch [24].

This exoskeleton weighs approximately 3 kg and has some levels of adjustability in order to adapt to the user body. In details, a custom fit can be achieved by regulating the hip, torso, shoulder and arms measures with sets of straps [22].

Different studies have analysed the efficacy of this exoskeleton. In particular, a recent study highlighted the different possible configurations for the tuneable parameters, concluding that these customizations have beneficial effects for particular tasks or workers when a suitable tuning is done on the end-user [24]. Another study highlighted a reduction in the rotator cuff activity and therefore concluded that the support provided by this device could help preventing the insurgence of WMSDs [22].

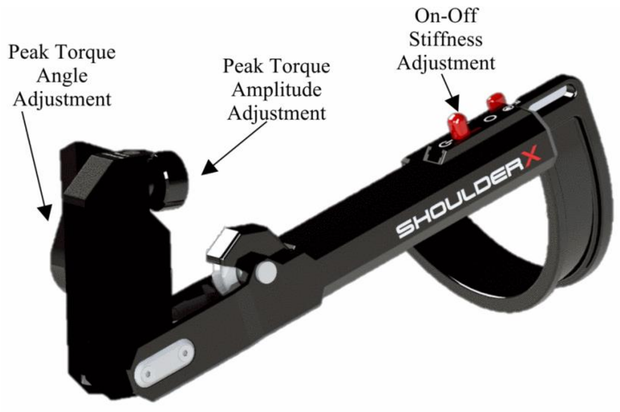

Figure 6: ShoulderX actuation mechanism with different possible adjustments [24] *© 2019 IEEE.*

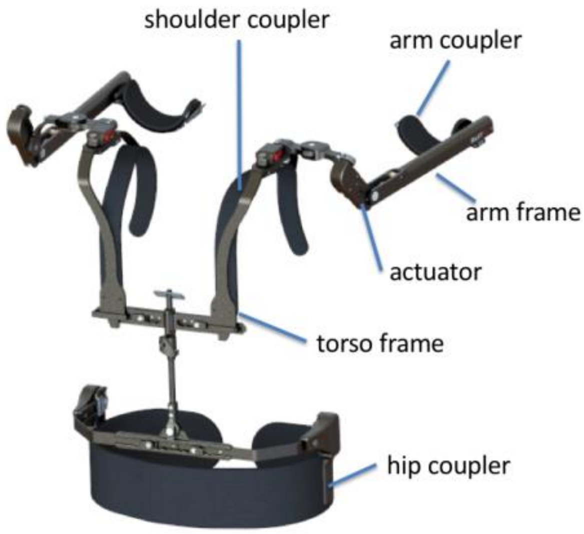

Figure 7: ShoulderX exoskeleton [22].

2.1.4 EksoVest

EksoVest (Ekso Bionics, Richmond, CA, USA) is an exoskeleton conceptually similar to its competitors, but it adopted a different mechanism around the shoulders. In particular, the momentum is generated around the shoulder and transferred to the arms cuffs by means of a hinge mechanism

[38]. In this way, this device does not have any shoulder pads differently from many other existing solutions, which make it appealing in all applications that are performed in hot environments. The movements are not impeded thanks to a patented stacked-link structure that follows the shoulder movements in the full range of motion proving the correct joint alignments.

The support increases gradually when the arms are raised and at the same time the supportive torque can be easily tuned off by the user [38]. The support level can be tuned by the user by swapping out the set of compact gas springs and the levels of assistance can be tuned differently for each arm.

The wearable exoskeleton has the possibility to be regulated to optimally fit the end-user, in addition it weighs 4.3 kg, which is slightly more than the competitors. The back pads and trunk length can be easily adjusted [38]. Moreover, unrestricted movements are allowed even for extreme body postures, like full overhead.

In recent years, some studies investigated the effectiveness of this device. A study analysed the device when it was firstly introduced in the market and simulated the tasks where the workers could possibly benefit from this exoskeleton. It was observed a reduced muscles activity and faster working, but also highlighted higher errors and the need of a training period for the workers to adapt to the wearable device [38].

2.1.5 SkelEx

SkelEx (Skel-Ex, Rotterdam, Netherlands) is a wearable robot conceived for light repetitive tasks and co-developed with various partners that started from the users' needs and feedbacks [39].

The structure of this wearable robot is made by a backpack-like structure, with the peculiarity of having two flat springs in the back (Figure 8). These springs can store the kinetic energy when the arms are lowered along the body, so that when the arms are raised again, the exoskeleton can assist the movement by providing a supporting torque. The support is given to the user thanks to padded cuffs that are positioned under each arm and that are directly connected to the back springs.

The device is able to adapt to the user movements and shape, allowing the shoulder to move freely. The energy stored is able to deliver a support to compensate the gravity effect on the arms, while transferring the forces to the lower part of the body. The exoskeleton weighs just 2.5 kg and has adjustable belt straps and hip belt [40].

This device originated from a study ordered by Skel-Ex industry. The aim of this trial was to analyse the critical movements and postures in order to produce an assistive device to reduce the upper body stress during job tasks [39]. The study concluded that the exoskeleton reduces the cardiac cost when following a repetitive protocol using short time tasks. The same authors conducted another study in order to implement a familiarization protocol to introduce the device to the users. They highlighted how the use of an exoskeleton is not intuitive thus the need for a familiarization protocol for better performance and acceptance [23]. Finally, a study investigated the effects of this device on muscles activation, showing that the shoulder muscle activations had significantly lower amplitudes when wearing the device [40].

Figure 8: SkelEx exoskeleton developed by SkelEx [41] *© 2021 IEEE.*

2.1.6 MATE

A last example worth mentioning is the wearable device developed by COMAU, an Italian company based in Turin and leader in the robotic automation field. In recent years, from a collaboration with IUVO, a spin-off company of Scuola Superiore Sant'Anna and Ossür, a worldwide leader in prosthetics, they developed a passive upper-limb exoskeleton called MATE (Figure 9). A first prototype called Proto-Mate was firstly tested, then the MATE was introduced into the market, and its latest model, MATE XT, has recently being commercialized.

The Proto-MATE was designed with the intent to assist workers in overhead tasks, together with a compact and lightweight design [27]. The exoskeleton has a human-machine interface (HMI), which is made of a back support structure and all the connections to the body, like the shoulder straps, arms cuffs and belt. The back structure is a T-shaped aluminium frame responsible for redistributing the forces from the arms to the pelvic area.

The torque box generator is the passive actuation component that includes two parallel elastic springs that can store energy and deliver it when needed for the assistance. The assistance is generated with a system of two connected gears, one coupled with the shoulder joint and the other not concentrically connected to the springs.

Figure 9: MATE exoskeleton design [27] *© 2020 IEEE.*

The support is not active when the arms are lying along the body, whereas it gradually increases when the arms are elevated. The MATE can be tuned to deliver four different discrete levels of assistance, all having a maximum delivery of support corresponding to the arms at 90 degrees. More adjustments can be made to fit the device to the worker, hence the back frame, width and straps on shoulder and belt allow to fit to the user.

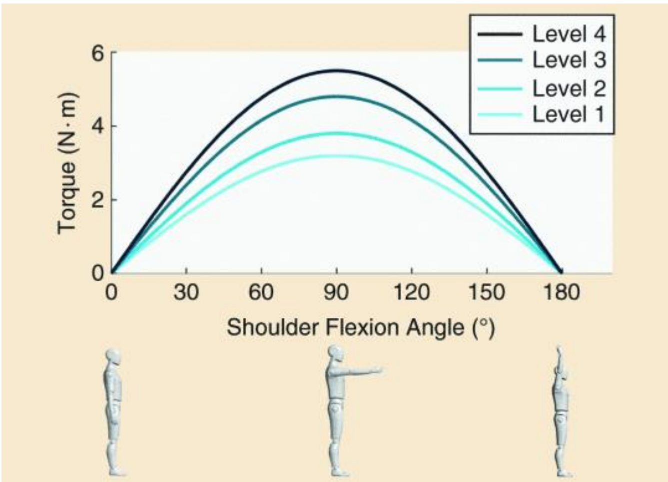

Figure 10: Torque profile of the assistance given by MATE exoskeleton during the flexion-extension of the shoulder [27] *© 2020 IEEE.*

The Proto-MATE weighs 3.5 kg and has a kinematic structure that was conceived with the intent to enable self-alignment to the human joint axes. The commercial version of the device (the MATE) weighs about 4 kg, while the last version, called MATE-XT, weighs from 3 kg to 4.5 kg (depending on the size) and has regulations to adjust the device on the worker [42]. The MATE-XT includes 8 levels of assistance and a redesigned mechanism to facilitate donning and doffing procedures (Figure 10). Moreover, a lighter carbon fibre structure is implemented as well as more resistant elements that make the wearable robot resistant to water, dust, UV and large temperature ranges.

The effectiveness of this device has been assessed by many studies. First of all, a preliminary study tested the pre-market version of the device, named Proto-MATE. This analysis highlighted a reduced physical strain in the shoulder muscles when performing simulated trials similar to assembly tasks [27]. Another recent work compared the MATE to other existing exoskeletons, Paexo and ShoulderX. The authors highlighted a similar reduction in muscle activity between the different models, with a slighter decrease in the muscles activation when using the Paexo. Overall, the devices gave similar benefits to the users, significantly reducing the effort needed for the simulated tasks [43].

2.2 ACTIVE SOLUTIONS

2.2.1 ABLE

In the field of active wearable robots, the challenge to design a device that correctly detects the user intentions is still an open challenge. Among the existing solutions, the French Atomic Energy Commission developed the ABLE 7-axes upper-limb exoskeleton (Figure 11). This device is conceived for industrial and medical applications, but it was at first used for post stroke patients as a rehabilitation tool [44].

The device is made of 7 non-anthropomorphic axes that can follow the arm human movements, also including a wrist part to carry a tool and orient it depending on the intended task [17]. Along the device, a haptic interface allows to have force feedback on the entire arm. The transmission system is based on the patented Screw and Cable System that uses a screw and a cable with a ball-screw to isolate the system from perturbative bending moments. Thanks to this solution, the system can have very low and stable dry friction and transfers in a highly linear way the obtained torque.

A crucial element in active devices is the controller, which for this robot was intended to be as transparent as possible. The two main functions for this control strategy are the dry friction and the weight compensation. The latter is designed to compensate the effect of gravity on the arm so that the user does not have to make any effort to keep the robot in a certain position.

The exoskeleton was tested on a static overhead screwing task [17]. The results highlighted a reduced mechanical energy and an increase in the cycle time when performing the task with the help of the ABLE exoskeleton. At the same time, this study only used three axes of the device during the defined task, suggesting that the minimum necessary number of degrees of freedom is still to be investigated.

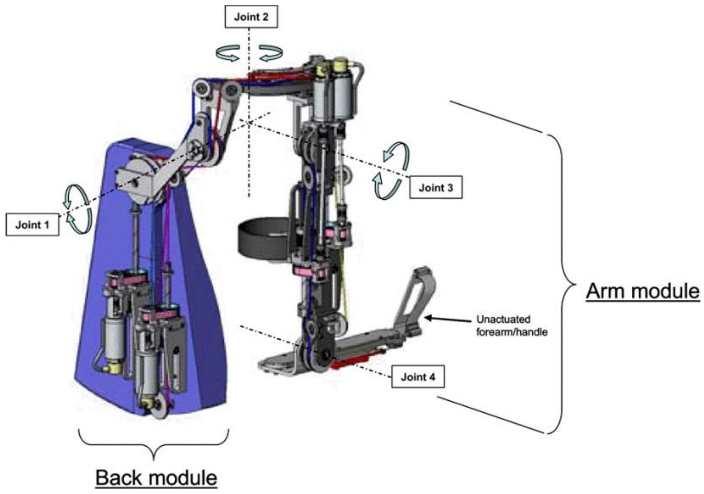

Figure 11: ABLE exoskeleton developed by the French Atomic Energy Commission [45].

2.2.2 LUCY 2.0

Among active exoskeletons, a recent work developed a hybrid active device called Lucy. The first model originated from the study of force paths along the body, assisting the upper arms and transferring the forces from the tool and arms to the pelvic area. A simple one degree of freedom structure was actuated with pneumatic cylinders and showed promising results in terms of pressure adjustability [37].

The mismatch between the human joints and the robot structure led to the creation of an improved version of the device, called Lucy 2.0 (Figure 12). This exoskeleton is a hybrid solution since it integrates both rigid and soft structural elements and both passive and active degrees of freedom. Concerning the actuation mechanism, a simple control scheme is implemented to regulate the pressure in a solenoid valve and therefore the support of the upper arm [37].

The control is based on different inputs, since the level of support is adapting during the work depending on the load and on the performed movements (Figure 13). In order to achieve this, three types of information are used to compute the desired support: the selected overall degree of support, the button at the tool tip to select additional support and a linear potentiometer that oversees the arm elevation. Afterwards, a pressure control loop controls the valves pressures depending on the computed pressure value. The obtained supportive torque is changing over the shoulder range of motion, reaching its maximum when the arms are elevated horizontally.

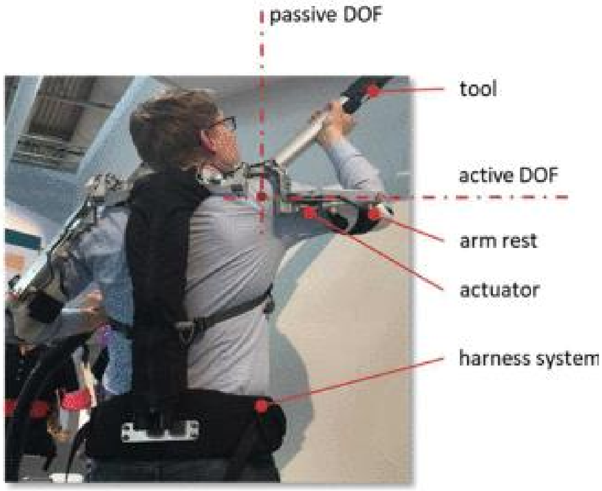

Figure 12: Lucy 2.0 exoskeleton [37] *© 2018 IEEE.*

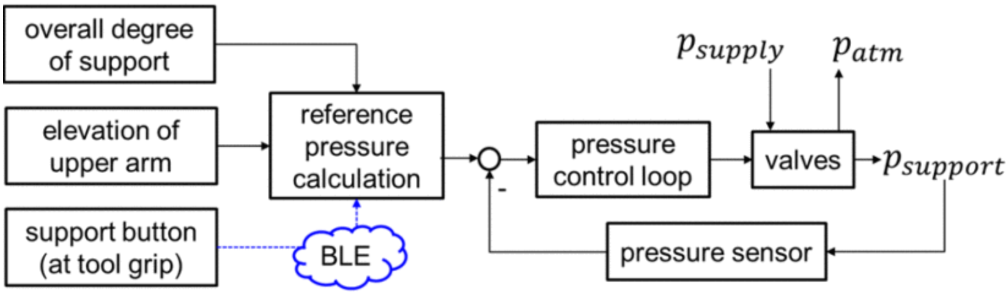

Figure 13: Control loop of the Lucy 2.0 exoskeleton [37] *© 2018 IEEE.*

A study analysed the benefits of this type of support, in order to investigate whether the benefits of a more complex active device could overcome the higher complexity. Different tasks were performed, such as fastening, screwing and grinding. The results showed that muscle activity was reduced when some tasks were performed with the help of the exoskeleton. On the other hand, other tasks did not show such high reduction, leading the authors to conclude that not all types of work would need an active exoskeleton. At the same time, participants in the study appreciated the presence of the button to control the exoskeleton, which is an important aspect when it comes to user acceptance of the device. Lastly, a stabilizing action was observed in the shoulder when using the device, implying the wearable robot led to both muscle activity reduction and joint stabilization [37].

2.2.3 Stuttgart Exo

A last example among active devices is the Stuttgart Exo-Jacket developed by the Fraunhofer Institute for Manufacturing, Engineering and Automation in Germany (Figure 14). The intent of this wearable device is to reduce the musculoskeletal injuries related to industry in both the logistics and montage fields [35].

The kinematic chain of the exoskeleton is conceived so that the range of motion of the upper body is not reduced and kinematic incompatibilities are avoided. In order to limit the micro misalignments between the wearer and the device, the active drive is placed on the shoulder. The exoskeleton has 12 degrees of freedom where only 3 are active. The remaining DOFs are passive and have spring mechanisms to compensate the weight of the device on the arm.

The actuation is performed with EC-motors and Harmonic Drives, so that overall, the structure is compact and can be easily mounted on the joints. The shoulder drive can generate a supportive torque up to 40 Nm, whereas the one for the elbow can reach 25 Nm. In the device, sensors are inserted to take measurements for the joint angle and speed. Moreover, force sensors can measure the force along the arm and on the user glove.

The main principle for this device, similarly to what happens with passive ones, is to transfer forces from the upper limbs to the hips and then to the ground. For this intent, a backpack-like structure is implemented and it can be integrated with a lower-limbs exoskeleton to transfer forces to the ground.

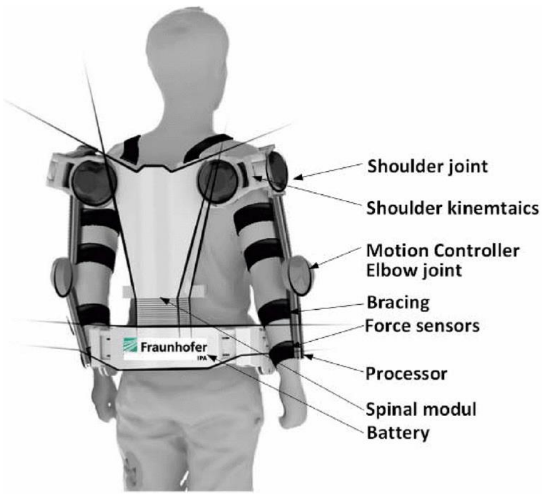

Figure 14: Stuttgart Exo-Jacket developed by the Fraunhofer Institute for Manufacturing, Engineering and Automation [35] *© 2017 IEEE.*

The control mechanism is not easy since automatic support detection and control is still an open challenge when designing active devices (Figure 15). In this case, firstly a state machine is used to recognize the states of the system and activate the proper high-level controller. Then, when the arm motion is recognized, a force booster acts as a force control to help the uplifting movement of the arm. A gravity compensation term acts in parallel so that the additional arm weight from gravity is added and compensated during the movement. It has to be underlined that a parameter identification procedure is necessary with a reference homing movement so that the control parameters can be tuned.

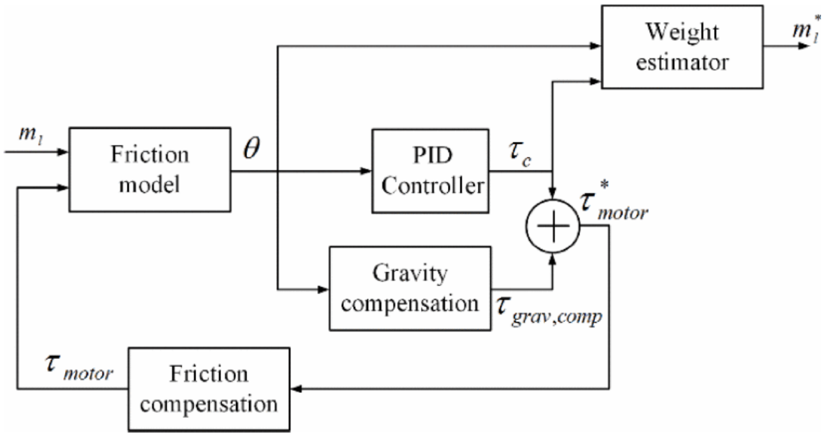

Figure 15: Control architecture of the Stuttgart Exo-Jacket [35] *© 2017 IEEE.*

A first design of this device analysed the control mechanism explained above. Moreover, a study highlighted the design features and the possible future use in industry of such wearable robot. At the same time, it suggested that the design process should take into account the ergonomic benefits as well as the comfort for the end-user [35]. Another recent study implemented a new control strategy on this exoskeleton, considering a force interaction control and automatic support control. The former produces a supportive torque from the estimation of the muscle force acting on the exoskeleton, whereas the latter is based on the gravitational compensation torque and the biceps muscle activations. Overall, the classification is based on Hidden Markov Models [46].

3 H-PULSE

In the wearable robots' field, passive exoskeletons for industrial applications are the most common solution and many models are nowadays commercially available. They can store the energy exploiting just passive mechanisms like springs or dampers and then deliver precise forces to the body [4]. It has been demonstrated that these devices can effectively relieve muscles from the required effort [30] and they do not require power nor control electronics [34], which implies lighter and safer solutions [4]. On the other hand, this kind of exoskeleton shows significant inertia [47] and it can lead to discomfort in case of joints misalignments. At the same time, antagonist forces may be necessary to return to the resting position [47].

Some studies have explored active exoskeletons, which usually include an adjustable level of support [37], [46]. The forces are delivered to the body by means of actuators that augment the human power and help in the joint's movements [25]. This field is promising but it still has some unresolved problems. The intention detection is still a difficult challenge [34], since it is not straightforward to give support to the user only when it is actually needed. Moreover, the automatic control of the support is still lacking a reliable approach [46] and the resulting structure can be too bulky and heavy for the end user [36].

In between the passive and active solutions, a new category can be introduced. Semi-passive devices can be designed to exploit low-power actuation units to modulate the behaviour of the passive spring mechanisms of passive exoskeletons and therefore provide exoskeletons with a certain degree of adaptivity to different tasks performed by the user [36]. In the state of art of industrial upper-limb exoskeletons, there exists just one solution implementing a semi-passive mechanism, which is the device used in this thesis work. The exoskeleton is the H-PULSE, a novel semi-passive upper-limb exoskeleton with motorized tuning of the assistive level [36]. The exoskeleton was developed by IUVO S.r.l. (http://www.iuvo.company, [48]), a spin-off company of Scuola Superiore Sant'Anna, within the H2020 HUMAN project (Grant Agreement n. 723737, website: http://humanmanufacturing.eu). The technology is patent pending [49].

The main design novelties implemented in the H-PULSE with respect to passive devices are an active tuning mechanism and integrated angle sensors. The former is composed of a spindle drive coupled with a servomotor allowing the automatic adjustment of the spring pre-tensioning which determines the assistive torque peak. The latter is represented by integrated sensors can estimate the user's shoulder kinematics in terms of the flexion-extension angle.

3.1 System description

The device is composed of the physical Human-Robot Interface (pHRI), the chain of passive degrees of freedom (DOFs), and the mechanism generating the assistance (called the active box). In this subsection, each part is described in details. The device weighs 5 kg and is conceived to have a safe and compact structure, to assure kinematic alignments and to avoid protruding parts.

3.1.1 pHRI

The pHRI is made of a T-shaped frame in aluminium alloy and adjustable pelvis and shoulder supports, making the device resemble a vest-like orthosis. In order to be comfortable to the user, the components in contact with the human body are padded with soft fabric (Figure 16).

The donning and doffing procedure is quick thanks to the pelvic belt. The stability on the iliac crest is guaranteed by an additional pair of straps that are fastened around the pelvic area (designed by Össur, Reykjavík, Iceland). The shoulders are stabilized with a strap linking the left and the right shoulder, which guarantees steadiness during the use. C-shaped cuffs are used to connect the user's arms to the active box on each arm and they can be tightened with Velcro straps.

Figure 16: H-Pulse pHRI [36] *© 2020 IEEE.*

3.1.2 Passive DOFs chain

When designing a wearable device, particular attention must be put in the degrees of freedom (DOFs) chain, which must be compliant with the physiological range of movement of the shoulder. The glenohumeral joint has three degrees of freedom: flexion-extension, abduction/adduction and internal/external rotation. Moreover, additional movements for the shoulder complex are the elevation/depression and protraction/retraction. Taking into account all these possible movements and to avoid to hinder the joint movements, a total of five DOFs is included in the design (Figure 17). A sliding joint (P1) is connected in series to a rotational joint (R1), both accounting for the adduction/abduction. The R1 is orthogonally connected to another rotational joint (R2) which, combined with P1, allows internal/external rotation and retraction/protraction of the shoulder. The chain continues with a rotational joint (R3), which is assisted by the action of the active boxes and allows the flexion-extension movement. A sliding joint (P2) is introduced in the arm cuffs linked to the active box. This last DOF is introduced to enable the exoskeleton to follow the vertical translational movement of the shoulder is case of high flexion angles.

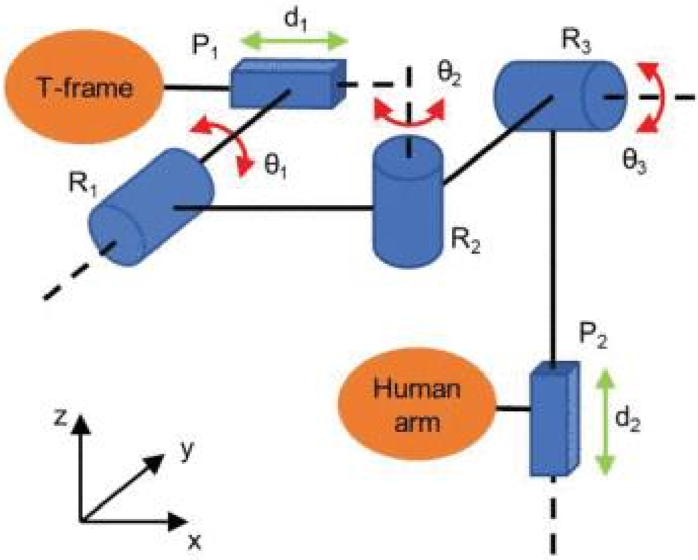

Figure 17: H-Pulse chain of passive degrees of freedom [36] *© 2020 IEEE.*

3.1.3 Active box

In order to generate the assistive torque, an active box is implemented in the exoskeleton (Figure 19). The actuation is composed of two gears: the shoulder gear in correspondence to the shoulder axis and the lever gear connected with the shoulder gear and with the carter of the active box with a spring. During the flexion-extension, the two gears move with respect to each other.

The connection of the spring is made in an eccentric way so that the generated torque is opposite to the gravity during the arm movement. Indeed, Figure 18 shows the angle-torque relationship: the shoulder flexion-extension angle in relation to the assistive torque has the same parabolic shape as the gravity acting on the human arm. The shoulder flexion-extension joint angle is measured through a 13-bit magnetic absolute encoder (RMB20, RLS®, Komenda, Slovenia). Moreover, the assistive torque is maximum at 90 degrees of flexion-extension and is null at 0 and 180 degrees. The spring is under tension on the whole range of motion of the arm (from -25 to 180 degrees) in order to avoid discontinuities in the torque profile.

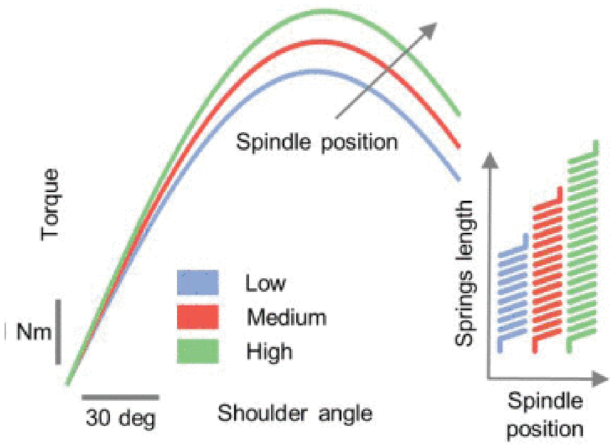

Figure 18: H-Pulse torque profiles generated by exoskeleton for different spindle positions [36] *© 2020 IEEE.*

The peak torque of the mechanism depends on the pre-tensioning of the spring and it can be varied from 4.5 Nm to 6 Nm. The pre-tensioning is set with a motorized system that enables an active and automatic tuning of the assistance level: the sled of one side of the spring can be moved with a spindle drive mechanism (GP 22S, reduction ratio: 333:1, Maxon Motor, Sachseln, Switzerland). The spindle drive is coupled with an 8W brushless motor (EC-max 16, Maxon Motor, Sachseln, Switzerland). The spindle has a 32-bit incremental encoder (Encoder MR Type M, 512 CPT, Maxon Motor, Sachseln, Switzerland), to measure the absolute position of the spindle drive from a given initial known position when the system is started up (homing procedure). For this intent, a Hamlin 55100 Hall sensor (Littlefuse Inc., Chicago, IL, USA) is used.

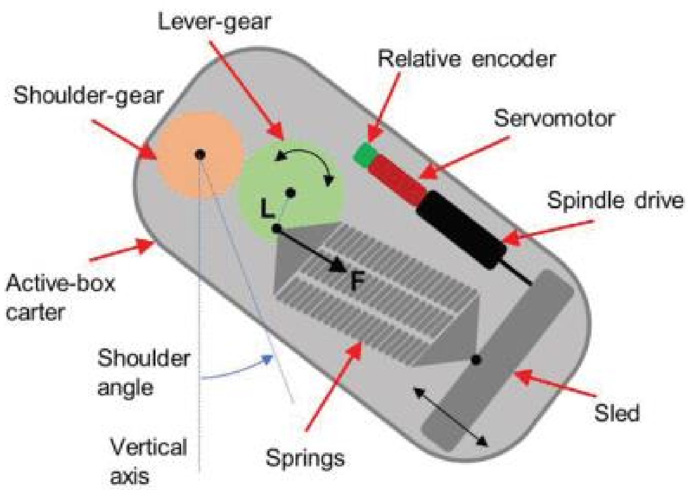

Figure 19: H-Pulse active box mechanism [36] *© 2020 IEEE.*

3.2 CONTROL SYSTEM

The control system of this device consists of a two-layer hierarchical architecture: a low-level control layer (LLCL) and a high-level control layer (HLCL). The control system runs on a NI system-onmodule (National Instruments, Austin, TX, USA), with a dual-core real-time ARM controller and a field programmable gate-array (FPGA) processor (Zynq-7020, Xilinx, San José, CA, USA). The two control layers are described in this section.

The LLCL runs on the FPGA at 1kHz and reads the sensors signals and drives the servomotors to set the pre-tensioning of the springs. A position control loop operates with a proportional controller that acts on the error between the desired position of the spindle drive (p_{des}) and the actual position (p_{act}). A bench test on the position controller obtained an average steady-state error lower than 0.02 mm. The output current for the servomotor is controlled with an Elmo Gold Twitter 15/100EE (Elmo Motion Control, Petach-Tikva, Israel).

The HLCL runs on the real-time ARM controller at 100 Hz and is responsible for the selection of the desired assistive level, corresponding to a precise pre-tensioning of the spring. Discrete levels of assistance are pre-set and can be chosen depending on the desired assistance required from the device. The number of possible discrete levels of assistance can be chosen in the design phase. In a first study on the H-PULSE, three possible discrete levels are implemented, namely low, medium, high, but it has been suggested that further studies can enlarge the choice to more discrete levels. This control layer has a graphical user interface that allows for the selection of the desired assistance level, the visualization and saving of the data [36].

This work aims at developing an innovative adaptive control algorithm for the automatic choice of the assistance level depending on the performed movement. The algorithm is implemented in the HLCL in order to automatically change the assistance level, without the need to manually select the assistance level before the use. The HLCL chooses the desired assistance level depending on the movements of the arms and feeds the information to the LLCL: the low-level layer is then responsible to change the spindle position in real time. Figure 20 shows the control layers architecture with the HLCL and the LLCL: the adaptive algorithm is implemented in the higher control level.

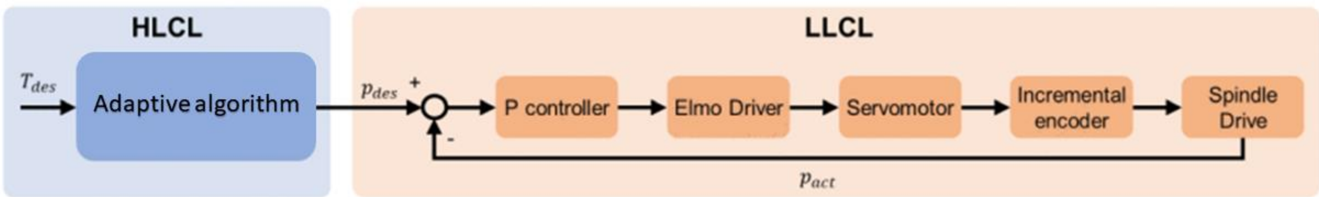

Figure 20: H-PULSE control layers, adapted from [36] *© 2020 IEEE.*

4 ADAPTIVE ALGORITHM

In the literature, passive exoskeletons are widely used and exploited in industry and have shown interesting results in reducing the physical strain and fatigue during demanding overhead tasks [4], [27], [38], [40]. Opening the way to new advanced solutions, the H-PULSE exoskeleton is an innovative semi-passive device with motorized tuning of the assistance. This exoskeleton is a research prototype, however it showed benefits in reducing the muscles' strain similarly to passive competitors. Indeed, a previous study has highlighted how the H-PULSE has a great potentiality in reducing both the muscles activity and the heart rate while performing prolonged static overhead tasks [36].

In passive devices, once the support level is determined it remains fixed at the set level for the whole duration of the work task. This aspect represents the main limitation of passive devices, since it has been suggested that that industry tasks are usually diversified and might need different support depending on the performed movements [4]. In the state of the art, control strategies for WR are widely studied for both active solutions [44], [46] and for soft robotics applications [34], [47], [50], whereas they are still to be explored for passive devices.

Some studies explored the possibility to implement regulations for passive devices. More advanced versions of passive exoskeletons have a certain number of settings that allows the regulation of the device support depending on the user biomechanical measures or performed task. For instance, the SkelEx exoskeleton presents a button to regulate the peak toque depending on the performed activity [24] and the Proto-MATE allows the choice between four discrete levels of assistive torque profiles [27]. Although promising, both these solutions implement changes that require a manual selection of the support, whereas to the best of the author's knowledge there is no current passive or semi-passive device implementing an automatic change of the support.

Therefore, the research is still open to find new solutions for the automatic control of the assistance. A clever strategy to determine the needed support could be implemented starting from kinematics information on the user movements. This concept is used for the design of the active exoskeleton Stuttgart Exo-Jacket, where the control loop takes as inputs the muscles activations and the arms movements [35]. This idea cannot be applied to passive devices, since they do not possess the electronics to implement this kind of control action. However, thanks to its semi-passive design, the H-PULSE can exploit the information on the user movements extracted from the sensors to adjust in real time the support level. The main goal of this thesis work is indeed the development and implementation of an adaptive real-time control strategy for the automatic selection of the assistance level of the H-PULSE exoskeleton. The developed algorithm is based on the observation of the task-related shoulder kinematics to automatically adjust the assistance the exoskeleton has to provide. This adaptability feature represents an innovative and promising way for the automatic online selection of the desired support level of exoskeletons.

When designing the algorithm, some considerations must be made in order to decide when a greater or smaller support is desired. Therefore, some hypotheses are made starting from biomechanical considerations and from previous studies on the shoulder movements:

- A passive exoskeleton can reduce the physical strain in both static and dynamic tasks [22]. However, during a static task, a higher level of support is preferred and it has been observed that it can significantly reduce the muscle strain [28], [40]. On the other hand, it has been observed that the triceps muscle, responsible for extending the shoulder in opposition to the exoskeleton support torque, increases its activation when higher levels of support are selected [22]. This implies that during more dynamic tasks, when the user has to contrast more the exoskeleton support, it might be preferrable to have a lower support in order to avoid possible activation of antagonist muscles.
- The most demanding position for elevated arms is when the shoulder flexion-extension angle is around 90 degrees. It must be recalled that the gravity acting on the arm during flexion-extension has a parabolic shape with a peak at 90 degrees [24], [27]. This aspect has to be taken into account when considering the needed support for static postures: the support has to be maximum around 90 degrees.

The challenge to develop an adaptive algorithm is still open in the research field. A first attempt to develop an adaptive algorithm for the H-PULSE has been previously done. Briefly, this algorithm considered the static or dynamic nature of the movement to set the desired level of assistance. However, although validation activities are still ongoing, preliminary results are promising, showing that the exoskeleton can provide different levels of assistance as the performed task changes. In this thesis work, a different approach was followed.

4.1 ALGORITHM LOGIC

The logic behind the developed algorithm is explained in this chapter. To command the desired assistive level by the exoskeleton, the proposed algorithm exploits the shoulder kinematic information measured by means of the exoskeleton integrated joint sensors. In particular, the joint angles and velocities are measured and stored in a 6-seconds buffer (i.e. time window), and used to extract the relevant features to compute the algorithm desired output, namely the assistance level that the exoskeleton provides during the next time window. These calculations are performed in the HLCL of the exoskeleton, while the desired assistance level is sent to the LLCL of the exoskeleton in order to change the position of the spindle, as shown in Figure 21.

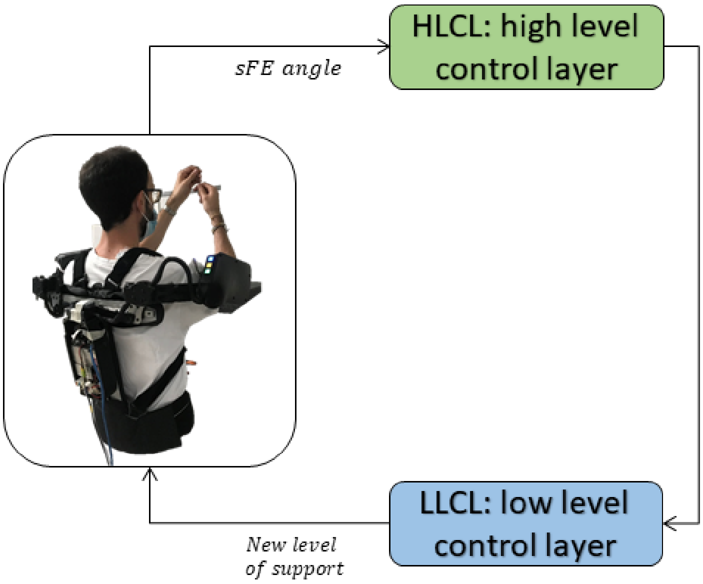

Figure 21: Control layers of the H-PULSE.

It is worth noting that there are seven possible discrete levels of assistance, each corresponding to a predefined pre-tensioning of the spring and thus to a precise position of the spindle. Table 1 shows the mapping between the discrete levels of support and the corresponding positioning of the spindle expressed in [mm].

Discrete levels	***Spindle positions [mm]***
Level 0	0
Level 1	2
Level 2	4
Level 3	6
Level 4	8
Level 5	10
Level 6	12

Table 1: Discrete levels and corresponding spindle positions in [mm].

The duration of the time window used for storing sensors data has been chosen taking into consideration the time needed by the actuation system to vary the springs length between two consecutive positions. In fact, the spindle drive takes approximately 5,5 seconds to change from one discrete level to the next, therefore covering a distance of 2 mm in the spindle position. When a new level of assistance is set, the system has to change at least one discrete level before a new level can be commanded.

Briefly, the proposed adaptive algorithm is composed of three major steps:

1) First, the absolute encoder reads the joint angles during the flexion-extension of the arm over a 6-seconds time window and extracts relevant features.
2) Second, calculated features are used to compute the outputs of cost functions.
3) Third, the cost functions contributions are used to compute the assistance level for the next time window, which is then saturated and discretized.

The following subchapters will describe in details each step of the adaptive algorithm developed in this thesis and that is schematically depicted in Figure 22.

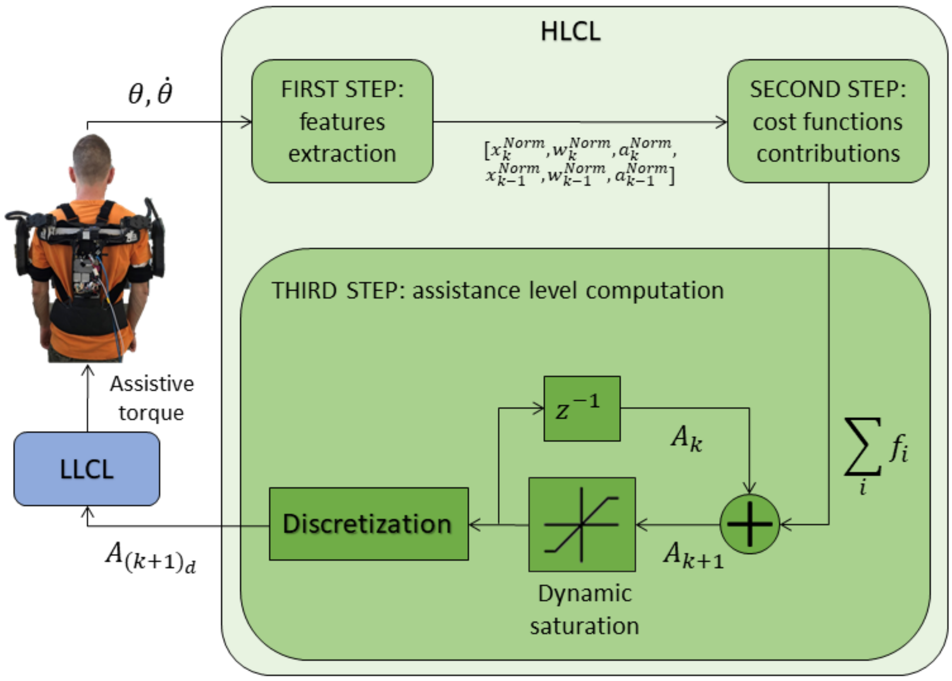

Figure 22: Adaptive algorithm control architecture.

4.1.1 First step: features extraction

In the first step of the algorithm, the encoder reads the angular position of the arms during the flexion-extension movements over a time window of 6 seconds. The shoulder flexion-extension angle (sFE angle) is sampled at 100 Hz and its values are collected in a 6-seconds buffer. From the joint angle (θ), the angular velocity ($\dot{\theta}$) is computed for the same time window and stored in an additional buffer.

Then, from the angular position and velocity buffers, different movement-related features are extracted. A feature is computed for a 6-seconds time window, therefore every 6 seconds a new value for each feature is calculated from the values stored in the buffers. The features are indicated with the appendix *k* since they are computed for the *k-th* time window and they are the following:

- x_k: sinusoidal function of mean sFE angle (mean value of θ buffer). This behaviour has been chosen so that this feature has a similar profile with respect to the torque one due to the gravity force acting on the arm during flexion-extension:

$$x_k = \sin\left(\frac{mean(\theta)}{180} * \pi\right)$$

- w_k: RMS (Root Mean Square) of the absolute value of the velocity. The RMS value of the $\dot{\theta}$ buffer is taken into account, since it can be used as an index of the energy associated with that signal:

$$w_k = \sqrt{\frac{\sum_{i=1}^{N} |\dot{\theta}_i|^2}{N}}$$

- a_k: amplitude of the movement, in terms of peak-to-peak distance. The maximum and the minimum value of the sFE angle in the θ buffer are subtracted to quantify the maximum excursion of the sFE angle over the chosen time window:

$$a_k = \max(\theta) - \min(\theta)$$

Then, the features values are normalized. The main reason behind the normalization is to have all the features varying within the same interval, chosen to be [0,1]. This point is of paramount importance in order to have in the final formula a linear combination of features all contributing with the same weight. For the normalization, the peak values are taken from experimental data or from biomechanical considerations, as follows:

- $x_k^{Norm} = x_k \in [0,1]$: by construction the used sine function is constrained in this interval. In particular, the maximum value of 1 happens when the sFE is around 90 degrees, whereas for sFE angles of 0 or 180 degrees the feature is zero.

- $w_k^{Norm} = \frac{w_k}{140\ deg/s}$: the peak value for the RMS of the velocity is chosen from experimental datasets. In fact, during experimental activities, the maximum value for the velocity RMS is about 140 deg/s in case of fast arms movements.

- $a_k^{Norm} = \frac{a_k}{180\ deg}$: the peak value for the amplitude is chosen from biomechanical considerations. In fact, during the flexion-extension movement, the arm can cover a maximum range of 180 degrees from the position where the arms are resting along the body to the maximum elevation of the arms above the head. Positions where arms are going behind the frontal plane are not taken into account since this case are not very common.

Finally, the features values for the *k-th* time window are collected and stored. In this part of the algorithm also the features from the previous time window, called *k-1*, are taken into account. The output matrix from this first step contains the 3 features for each of the time windows *k* and *k-1*:

$$[x_k^{Norm}, w_k^{Norm}, a_k^{Norm}, x_{k-1}^{Norm}, w_{k-1}^{Norm}, a_{k-1}^{Norm}]$$

4.1.2 Second step: cost functions contributions

In the second step of the algorithm, the features computed for time widows *k* and *k-1* are used inside cost functions. The outputs of each cost function are then summed together to obtain an overall sum called $\sum_i f_i$.

For the computation of the cost functions, two different approaches have been explored. In both cases, the main intent was to obtain a sum of the cost functions contributions ($\sum_i f_i$) that can be used in the computation of the assistance level for the next time window.

4.1.2.1 P-like formulation

The first approach explored was the P-like (proportional) formulation. In this formulation, only the features from the *k-th* window are considered. The functions for the computation of the sum of cost functions contributions are the following:

- $x_k^{Norm} \in [0; 1]$
- $w_k^{Norm} \in [0; 1]$
- $a_k^{Norm} \in [0; 1]$

The *proportional* definition came from the fact that only the terms from the last time window are taken into account. The final linear combination of the features is the following:

$$\sum_i f_i = x_k^{Norm} - w_k^{Norm} - a_k^{Norm} \tag{1}$$

The signs of each term of Equation (1) are set according to the desired contribution of each feature. For the x_k^{Norm}, that considers the mean sFE angle, a positive contribution is needed since when the arms are elevated a greater support is desired. The w_k^{Norm} and a_k^{Norm}, on the other hand, have a negative contribution since these two features indicate a dynamic movement. During this kind of actions, a lower level of support is wanted since the exoskeleton does not have to impede the movements when the user performs a fast (high w_k^{Norm}) or ample (high a_k^{Norm}) movement.

This first implementation showed promising results with a relatively simple formulation. However, it considers only what happens in a certain time window, thus it can sense less the changes in the system behaviour and the algorithm output is slower in following the system evolution. These limitations were overcome with a more detailed formulation that considered also the values of the features from the previous time window (*k-1*).

4.1.2.2 PD-like formulation

The second implementation was called PD-like (proportional-derivative). In this case, the features from both time window *k* and time window *k-1* are considered. Therefore, also the feature variation from *k-1* to *k* is taken into account to consider the feature evolution over two consecutive time windows. This is the reason behind the naming of this formulation: proportional terms are considered (features in *k*), but also derivative contributions (features variations from *k-1* to *k*).

The cost functions contributions in this case are the following:

- $x_k^{Norm} \in [0; 1]$
- $w_k^{Norm} \in [0; 1]$
- $a_k^{Norm} \in [0; 1]$
- $x_k^{Norm} - x_{k-1}^{Norm} \in [-1; 1]$
- $w_k^{Norm} - w_{k-1}^{Norm} \in [-1; 1]$
- $a_k^{Norm} - a_{k-1}^{Norm} \in [-1; 1]$

These cost functions contributions are linearly combined in the following way (2):

$$\sum_i f_i = x_k^{Norm} + (x_k^{Norm} - x_{k-1}^{Norm}) - w_k^{Norm} - (w_k^{Norm} - w_{k-1}^{Norm}) - a_k^{Norm} - (a_k^{Norm} - a_{k-1}^{Norm}) \tag{2}$$

Similar to the previous formulation, the signs of Equation (2) are chosen according to the desired contribution. For the x_k^{Norm} proportional and derivative terms a positive contribution is needed. The assistance level is increased in case the arms are elevated (proportional term contribution) or when there is an increase in the arms elevation (derivative term contribution).

For what concerns w_k^{Norm} and a_k^{Norm}, their proportional and derivative parts both have a negative contribution. In case a dynamic movement is performed (proportional term contribution) or starting (derivative terms contribution), a negative contribution is wanted. In fact, during more dynamical tasks a lower level of support is desired since the exoskeleton does not have to hinder the user.

This second version (Equation (2)) of the algorithm showed some advantages with respect to the previous implementation (Equation (1)). In particular, it is faster in adapting to the system evolution in time, more responsive to system changes, and more accurate to follow the system behaviour. This behaviour is related to the more detailed formulation, with proportional and derivative contributions.

4.1.3 Third step: assistance level change and dynamic saturation

In this third and last step, the level of assistance for the next time window is decided. The values needed for this step are the sum of the cost functions contributions $\sum_i f_i$ and the currently commanded assistance level A_k. The first is obtained from the computations described above (Equation (2)), whereas the latter is the assistance level computed in the previous time window (in *k-1*) and then commanded to the system for the *k-th* time window.

The assistance level for the next time window (*k+1*) is computed according to the following relation (3):

$$A_{k+1} = A_k + \sum_i f_i \tag{3}$$

This simple computation implements a finite difference equation. In fact, Equation (3) is a linear combination of features from consecutive time windows. The level A_k is a value computed in the previous time window that considered the values in *k-1* and *k-2*, whereas the sum $\sum_i f_i$ is obtained from a linear combination of features in *k* and *k-1*. This aspect allows to have a formulation that takes into account the system history and its variations over time.

During the development phase of the algorithm, a limitation of the proposed formulation was encountered. As a matter of fact, in case of a stationary static condition, A_{k+1} always increased and reached the maximum assistance level, regardless of the mean sFE angle. However, this behaviour was not desirable; it was indeed preferred to have a value of A_{k+1} that in stationary conditions takes into account the value of the sFE angle, namely the angular value around which the movement is performed.

To tackle this problem, a dynamic saturation of the assistance level was therefore implemented: the maximum value for A_{k+1} is given by dyn_sat, which depends on the mean sFE angle of the last observed window according to the following relation (4):

$$dyn\_sat = 6 * \sin\left(\frac{mean(sFE)}{180} * \pi\right)^2 \tag{4}$$

Equation (4) was built with the goal of having a sinusoidal profile for the dynamic saturation. In fact, this function shape recalls the parabolic profile of the gravity torque acting on the arm during flexion-extension. Indeed, the maximum reachable assistance level depends on the sFE angle and thus the required gravity torque that the exoskeleton has to compensate during the elevation of the arm. Moreover, Equation (4) is elevated at the power of 2 so that the shape of this function is less steep than a simple sine. In fact, the intention was to have the lowest assistance for angles below 20 degrees or above 160 degrees, similar to the approach in [24]. Therefore, after the computation of the assistance level A_{k+1} according to Equation (3), its value is saturated at a value given by dyn_sat (Equation (4)).

As a final step, the discretization of the computed assistance level is performed. In fact, the possible assistance levels that can be commanded to the system are seven discrete values (Table 1). The mapping from the continuous to the discrete value is made with the nearest integer approximation (i.e. 5.5 is 6 and 4.2 becomes 4). The discretized assistance level $(A_{k+1})_d$ is then passed to the LLCL that is responsible for the spindle drive movement according to the commanded level.

4.2 OFFLINE IMPLEMENTATION OF THE ALGORITHM

The algorithm was first implemented and tested offline in the MATLAB R2019b (The MathWorks, Natick, MA, USA) environment, where some datasets are used to analyse the algorithm behaviour. In particular, this chapter reports some relevant datasets examples along with comments on the corresponding algorithm behaviour.

A first test was done with a varied dataset to see the evolution of the algorithm output in case of a sequence of diverse movements (both dynamic and static) at different sFE angles. Figure 23 shows the sFE angle behaviour and the corresponding algorithm values.

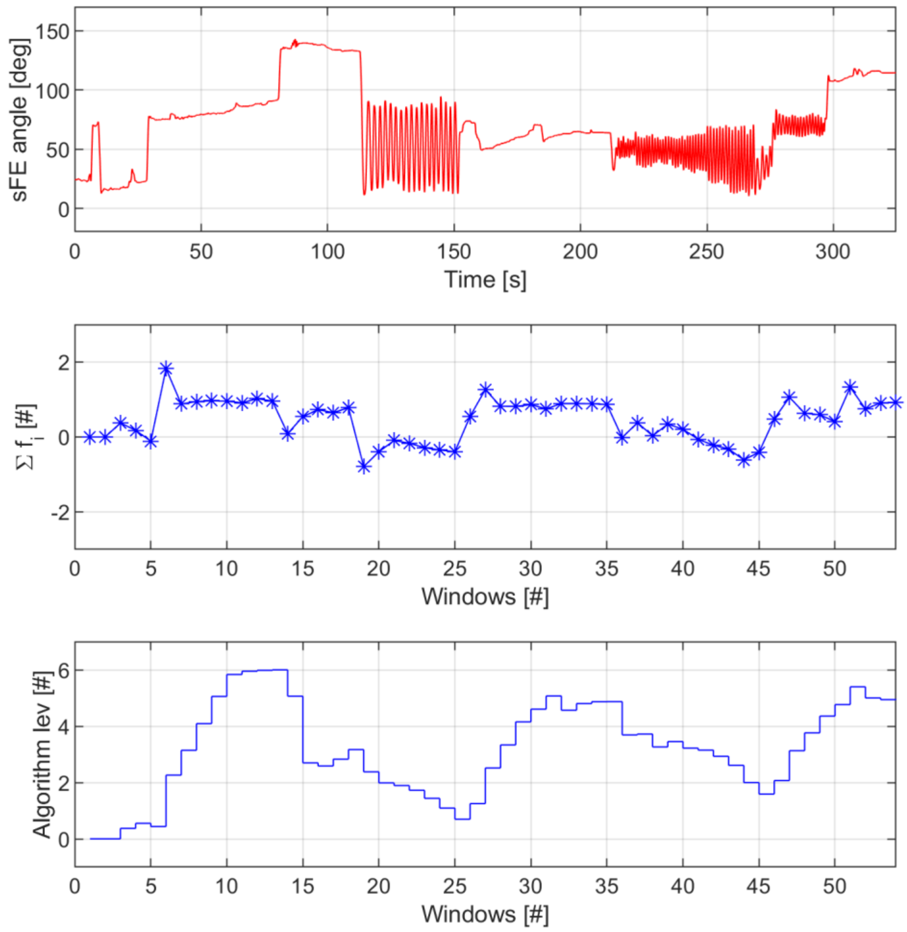

Figure 23: Adaptive algorithm behaviour on a given dataset.

The algorithm accurately follows the system behaviour in time. In fact, the sum of cost functions contributions ($\sum_i f_i$) depicts what is happening in the system: for more static movements it has a positive value. On the other hand, in case of more dynamic movements, the cost functions sum is a negative value. This results in an overall assistance level that is greater in case of static tasks, whereas it is lower when a dynamic task is performed.

It is interesting to analyse also each cost function contribution behaviour with respect to the system evolution. Figure 24 shows each cost function and its behaviour in time, with the proportional contribution (*k* appendix), as well as the derivative contribution (*k-1* appendix). An important difference can be remarked for proportional and derivative terms. Proportional terms can assume similar values for consecutive windows, since they describe what is happening in a certain time window and the system can maintain the same value for consecutive time windows. On the other hand, derivative terms tend to have spikes and less constant values. This is due to the fact that they describe system variations over consecutive time windows, so they assume a certain value only when the system is changing, whereas in stationary conditions the derivative terms are zero.

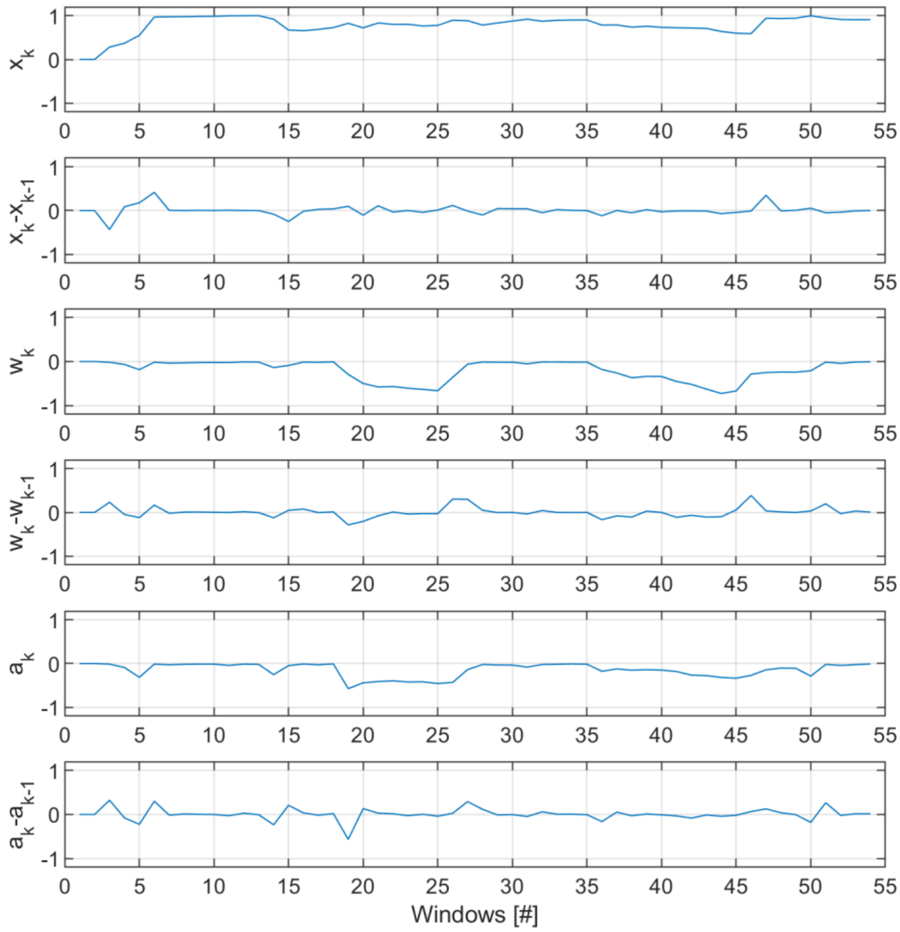

Figure 24: Cost functions contributions behaviours.

As a last step, the support level obtained from the algorithm has to be discretized. The mapping to the discrete values is shown in Figure 25: both continuous (A_{k+1}) and discretized $(A_{k+1})_d$ values are shown.

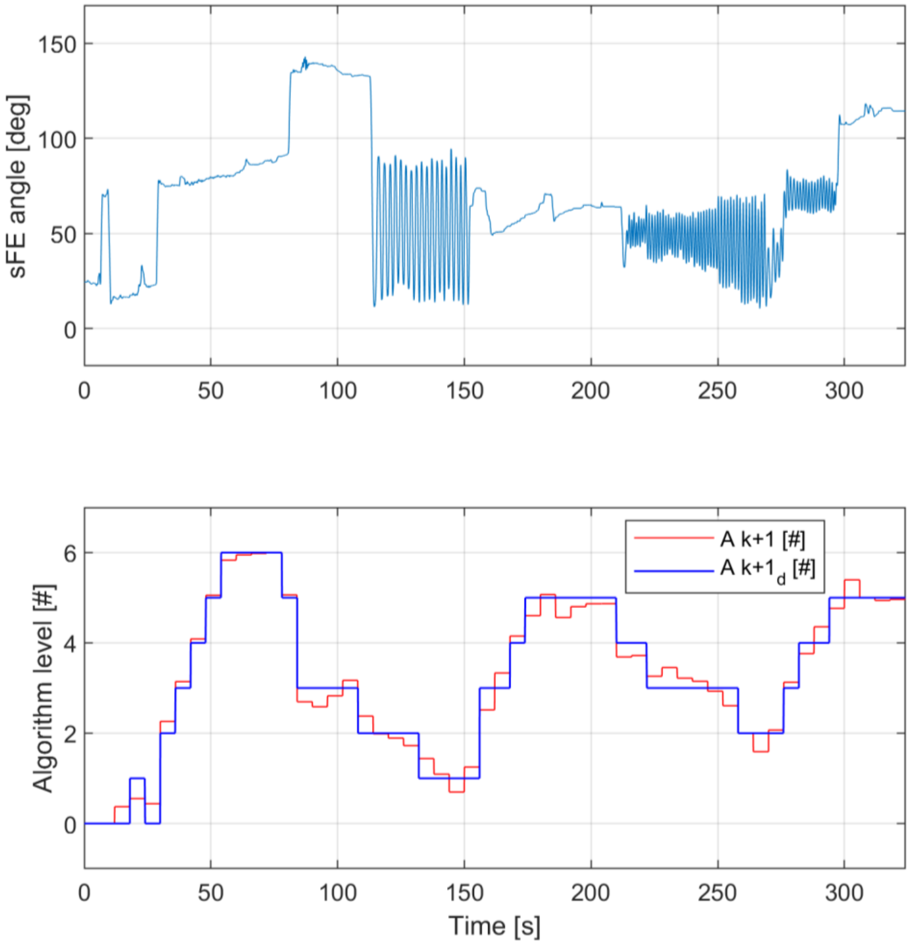

Figure 25: Algorithm output value and discretized value.

Another aspect that has to be underlined is the dynamic saturation action on the system output. This function is introduced as upper limit for the computed assistance so that the maximum reachable support depends on the sFE angle. It can be seen that the algorithm reaches the maximum level of 6 only when the sFE angle is around 90 degrees. On the other hand, when the sFE angle is not around 90 degrees, the dynamic saturation cuts the algorithm level to a level lower than 6. Figure 26 highlights the dynamic saturation with respect to the algorithm maximum reached level. For instance, for sFE angle values of 140 degrees the maximum value is 3, whereas for sFE values of 70 degrees the maximum level is 5.

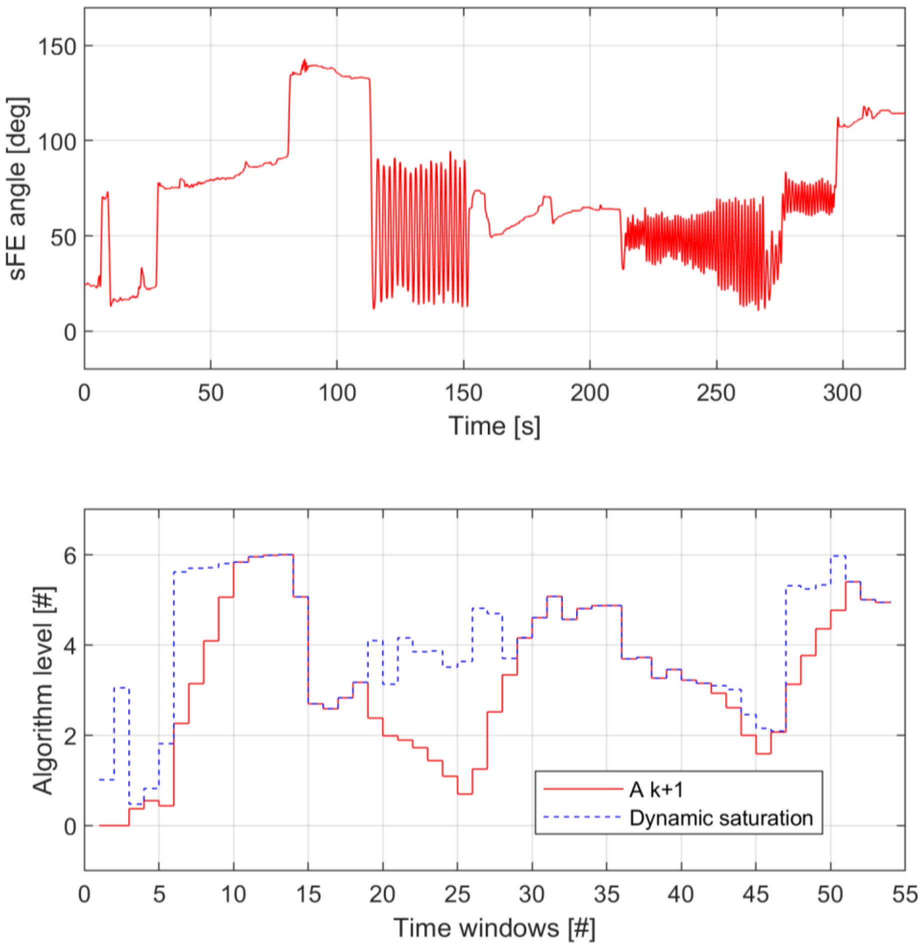

Figure 26: Dynamic saturation action on the maximum reachable level.

As a second trial, a more structured set is analysed. In this case, static and dynamic tasks at different mean sFE angles are put in sequence to examine how the algorithm can adapt to the system behaviour. The chosen sequence is static-dynamic-static and each subsequence is repeated at three different shoulder elevation angles.

Figure 27 shows the resulting assistance level computed by the algorithm. As expected, for more static tasks the support level is greater, whereas for more dynamic tasks the support level decreases until it reaches the minimum value. The dynamic saturation action can be seen for static tasks at 120 and 60 degrees, where the maximum support level is around 4.

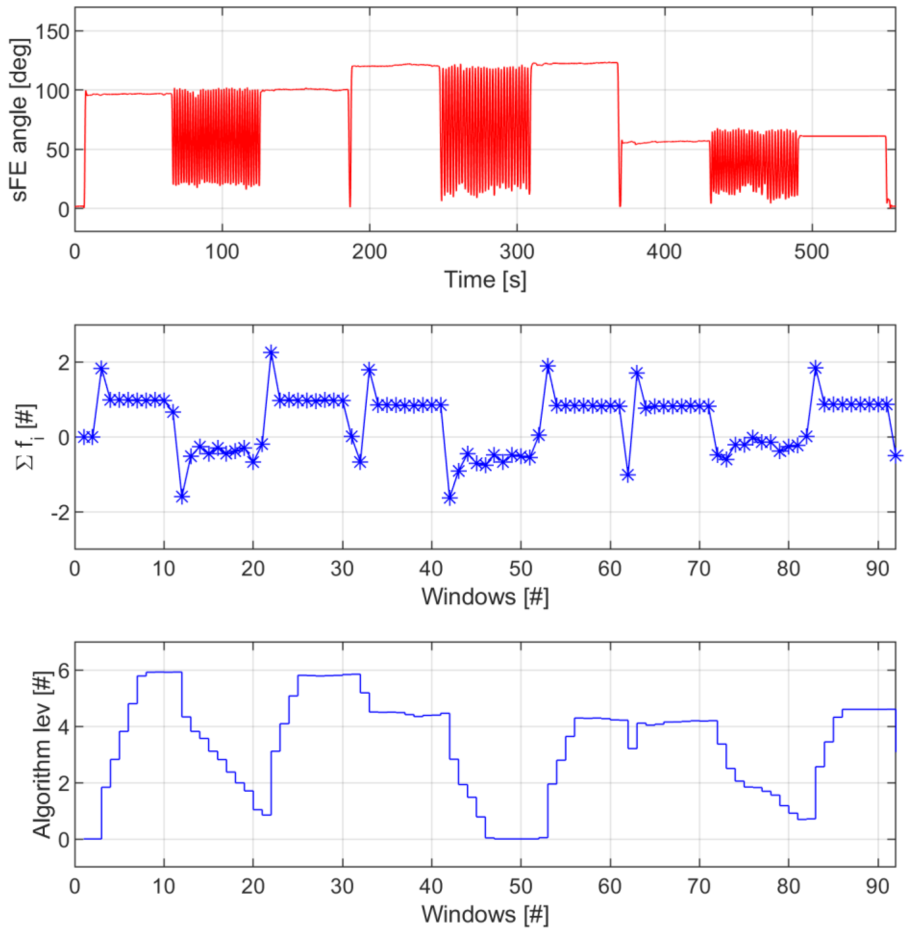

Figure 27: Algorithm behaviour on a given dataset.

The discretized values that are commanded to the LLCL are shown in Figure 28.

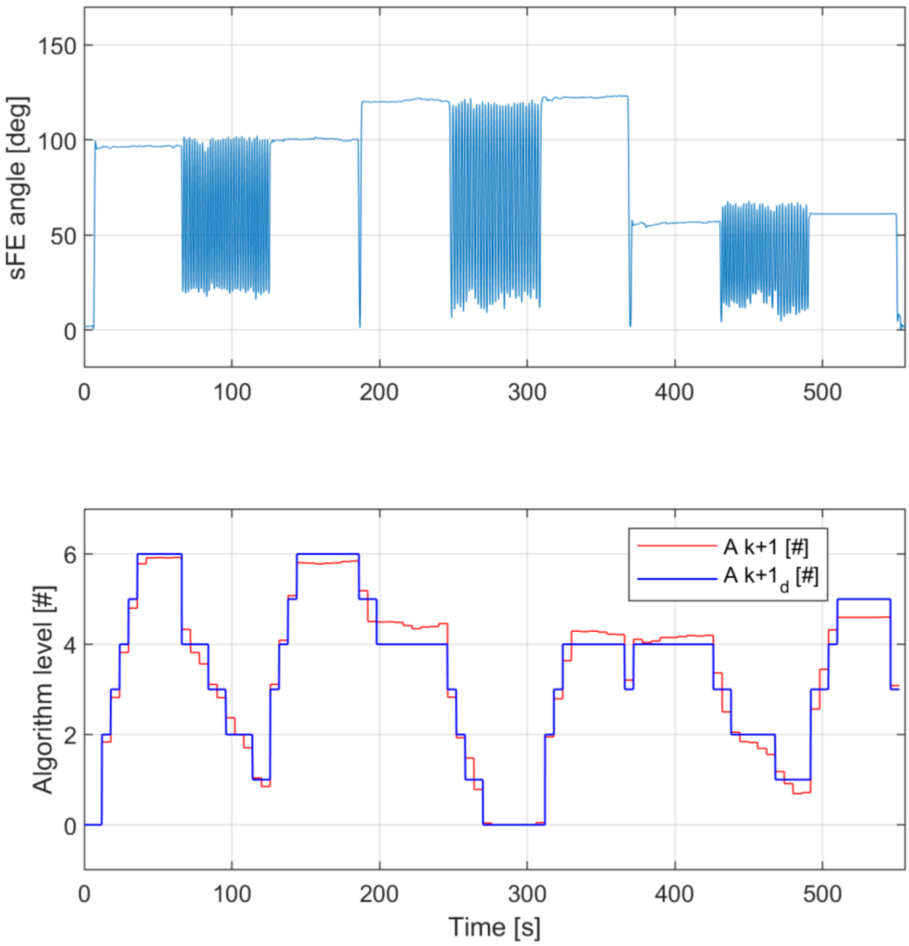

Figure 28: Algorithm output value and discretized value.

4.3 Real-time simulations

Following the algorithm offline development in MATLAB, the upcoming step was the real time implementation on the exoskeleton control system. Before integrating the algorithm in the real-time processor of the exoskeleton, it was necessary to test its real-time performance by means of a simulator. The simulator was developed in the same programming language used in the H-PULSE, namely LabView 2018 (National Instruments, Austin, TX, USA).

Figure 29 below briefly resumes the main steps of the LabView code to implement the algorithm. It can be remarked that the steps and logic of the real-time code reflects the same steps used in the algorithm development.

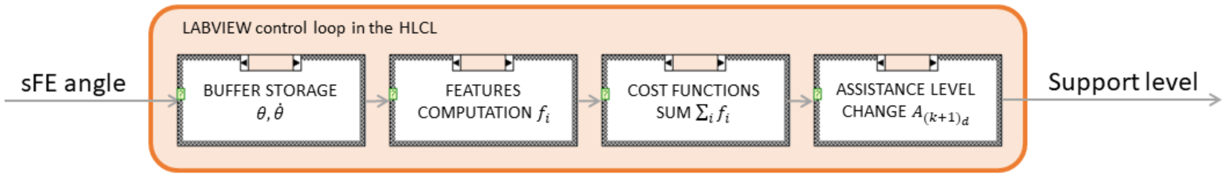

Figure 29: LabView control architecture.

4.4 ALGORITHM MATLAB AND LABVIEW COMPARISON

In order to assess the correctness of the LabView implementation, the algorithm output obtained from LabView is compared to the MATLAB one. This is implemented thanks to a custom MATLAB routine that over-imposes the two outputs to check their similarity. Figure 30 show an example of the validation of the LabView code. It can be seen that the algorithm output is the same in the offline MATLAB version and in the real-time LabView simulation, meaning that the algorithm is correctly implemented in LabView.

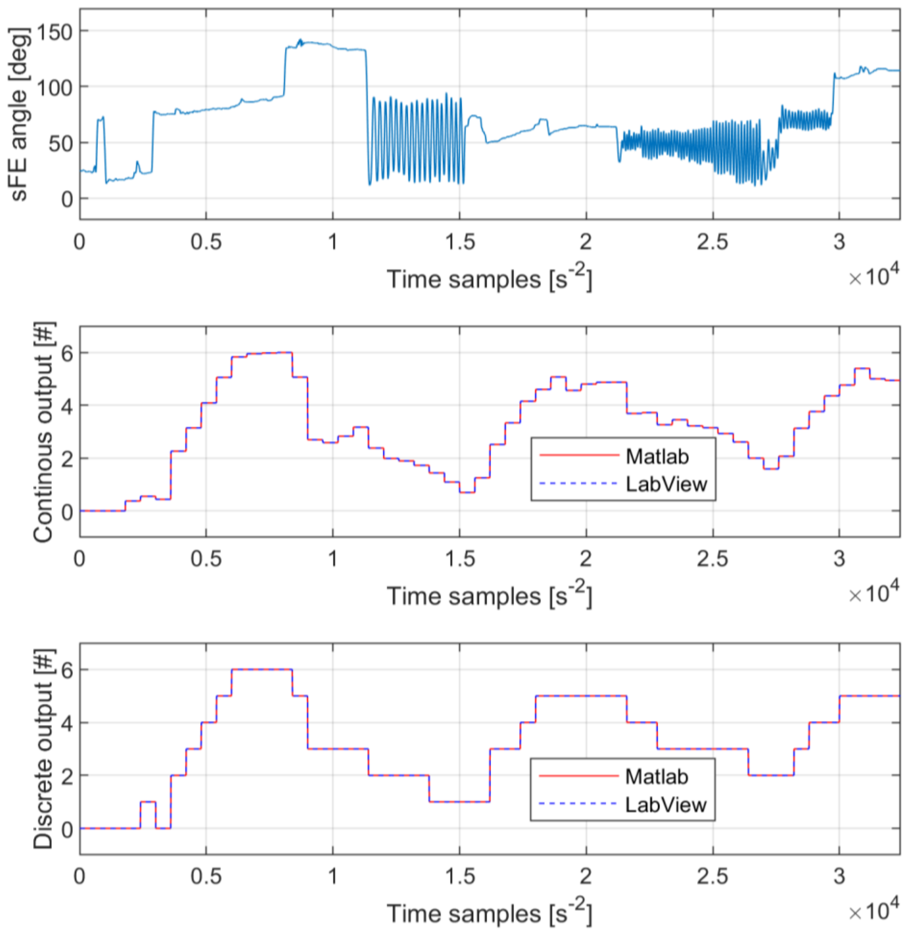

Figure 30: MATLAB and LabView algorithm outputs for a given dataset.

5 EXPERIMENTAL ACTIVITIES

The previous chapter described the development of the adaptive algorithm for the real-time computation of the assistance level for the semi-passive upper-limb exoskeleton. The design process, composed of the offline development performed in MATLAB and the LabView simulation, was followed by the algorithm validation with human-in-the-loop experiments. In order to perform this step, the algorithm was implemented in the real time LabView code of the exoskeleton and experimental activities were carried out.

The objective of this experimental trial was to analyse how the user can benefit from the H-PULSE support when the level of assistance is set and changed in real-time according to the adaptive algorithm. To perform proof-of-concept evaluations, two subjects were recruited to wear the exoskeleton and perform a pre-defined sequence of simulated manual working tasks.

In order to investigate the effects of the adaptive control strategy, the adaptive algorithm condition (AD-EXO) is compared to two other conditions. In particular, one condition contemplates the case where the exoskeleton is not worn by the user (namely NO-EXO condition), whereas the other case considers the exoskeleton worn by the user with a fixed assistance (FIX-EXO). The fixed support level is computed prior to the start of the experiment in order to provide a torque which can compensate approximately 50% of the gravity torque acting on the arm, estimated from considering the height and weight of each subject, similar to approach adopted to determine the assistance level of the passive exoskeleton MATE [27].

5.1 METHODS

5.1.1 Experimental tasks and setup

When deciding the tasks that the user has to perform in the experimental trials, it is of paramount importance to make some preliminary considerations. In fact, considering the algorithm responsiveness and the system time constant, some specific requirements must be followed. First of all, a task should last about two minutes to observe a transient phase and a stationary phase of sufficient length to perform EMG analysis. Moreover, tasks of different nature, namely dynamic and static, are alternated within the same sequence to analyse how the adaptive algorithm output can reflect the system changes over time. In order to address these points, a sequence of three tasks was identified, where static, dynamic and semi-dynamic movements were performed in order. Each task lasted 2 minutes and they were performed sequentially by the subjects for a total duration of 6 minutes. The movements were inspired by real working activities, with the goal of simulating possible applications of the exoskeleton in industry environments.

Table 2 resumes the chosen tasks and their main characteristics.

Task	***Mean angle [deg]***	***Type***	***Duration [min]***
Screwing	~90	Static	2
Box handling	~45	Dynamic	2
Wall painting	~120	Semi-dynamic	2

Table 2: Chosen tasks and main characteristics.

For the tasks sequence execution, a dedicated setup was prepared and equipped to perform the experimental tasks. A structure with shelves at different heights was used to have the different working conditions. In order to have the actions performed at the correct shoulder angles, the shelves height could be adjusted in function of the height of the subject. Figure 31 shows the setup for the experiments as well as the tools used for the different types of tasks.

Figure 31: Experimental trials setup structure, with the screw for the static task (1), the box for the dynamic task (2) and the roll for the semi-dynamic wall-paint task (3).

Figure 32 shows one of the subjects performing the movements chosen for the sequence.

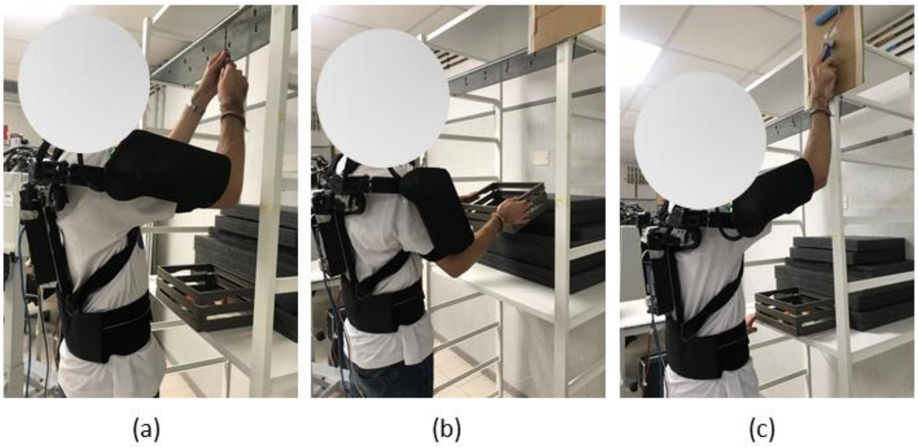

Figure 32: Movements performed in the experimental trial. (a) – static screwing, (b) – dynamic box handling, (c) – semi-dynamic wall painting.

5.1.2 Preliminary test

In order to test the experimental procedures, an experimental trial was performed to analyse the algorithm behaviour when this sequence of tasks is executed. Figure 33 shows the sFE angle behaviour of the three performed tasks as well as the corresponding algorithm output.

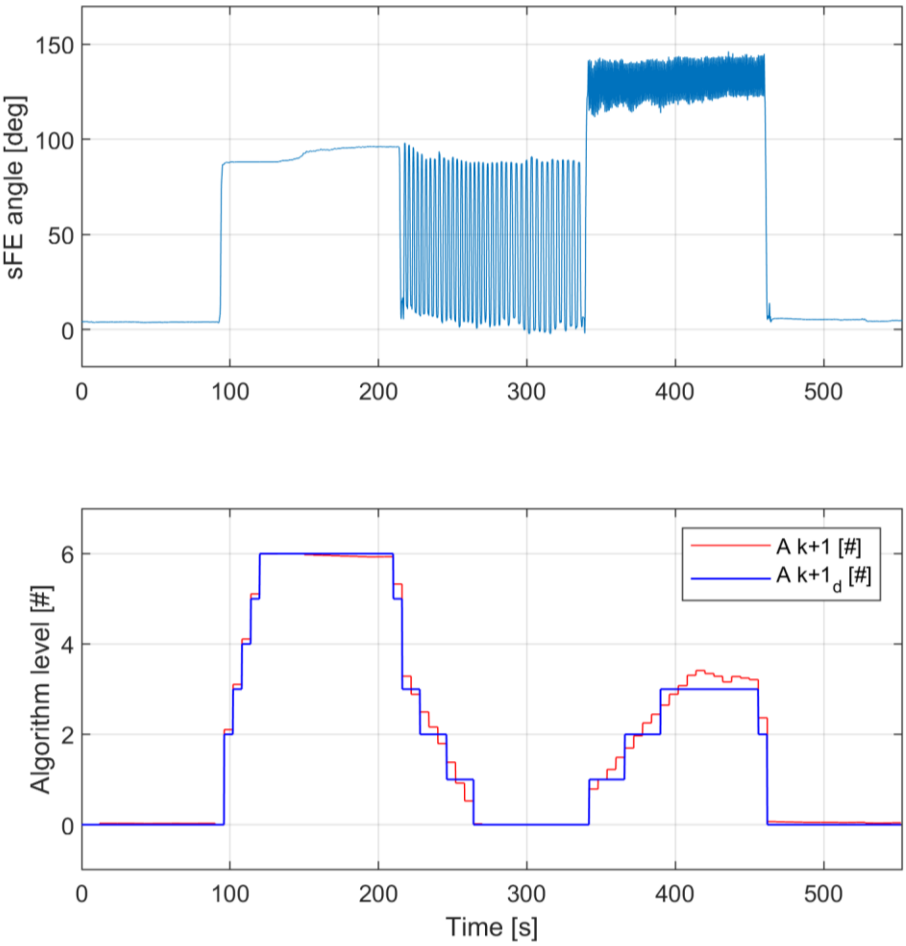

Figure 33: Experimental dataset and corresponding adaptive algorithm behaviour.

Overall, the behaviour of the algorithm is the one expected. The support level increases for static tasks performed at angles around 90 degrees, reaching at steady state the maximum assistance level of 6. Conversely, the assistance decreases when the dynamic task is performed, until it reaches the minimum level of 0. These results highlight a first difference with respect to a fixed assistance level condition: when performing a static task, the adaptive condition leads to the maximum value of assistance 6, which is usually higher than the fixed level. Conversely, in case of dynamic task, the adaptive algorithm output at steady state is 0, in most cases lower than the pre-chosen fixed level. An interesting behaviour is remarked when the semi-dynamic task is performed, the assistance level increases again but it does not overpass the value of 3. In fact, the maximum level reached by the algorithm depends on the sFE angle: for angles of 90 degrees, the maximum reachable support is 6, whereas the semi-dynamic task is at higher angles therefore the maximum reachable level is 3.

These differences in the provided support level can result in possible changes in the observed physical strain of the user in the different conditions. The experimental trials aimed indeed at highlighting how the observed user effort, in terms of muscular activity and heart rate, can change depending on which of the three conditions is tested.

5.1.3 Efficacy assessment

The main objective of the experimental trials was to investigate the effects of the adaptive control strategy against the conditions where the exoskeleton delivers a fixed level of support or where no exoskeleton is worn.

In order to evaluate the efficacy of the adaptive algorithm, two different objective measures were considered, namely surface electromyography (EMG) for assessing changes in localized muscular strain and heart rate (HR) to assess changes in global fatigue. The main goal of this analysis was to investigate possible differences in these metrics among the three considered conditions (i.e. NO-EXO, FIX-EXO, AD-EXO).

Among all the shoulder muscles, the EMG signal was recorded from the muscles that are more involved during the flexion-extension movement. Indeed, EMG sensors were placed on the anterior deltoid (AD), the medial deltoid (MD), the posterior deltoid (PD), the upper trapezius (UT), the triceps brachii (TB), and the latissimus dorsi (LD), as shown in Figure 34. To record a clean ECG signal, a probe was attached to the chest, in the left rectus abdominus: such location was identified as the most practical for the collection of the ECG signal, due to the proximity to the heart and the cleanliness of the recorded trace from which the HR was then computed. Finally, an additional probe was placed on the exoskeleton and used for the synchronization between the EMG signals and the exoskeleton data, as previously done in [36].

All the electrodes were placed on the muscles according to the SENIAM protocol [51], as shown in Figure 34 and Figure 35. The EMG signal is collected just for the right side of the body, since a previous study on the H-PULSE highlighted that the muscle activity is the same for both sides when symmetric tasks are performed [36].

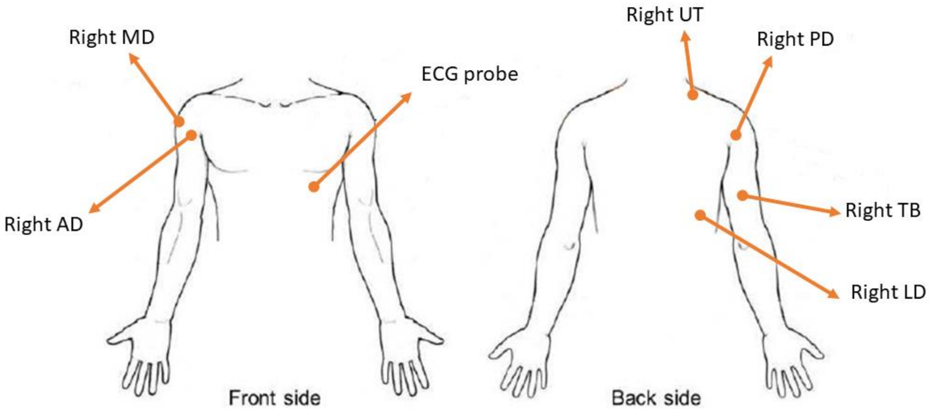

Figure 34: EMG probes location and corresponding muscles, adapted from [36].

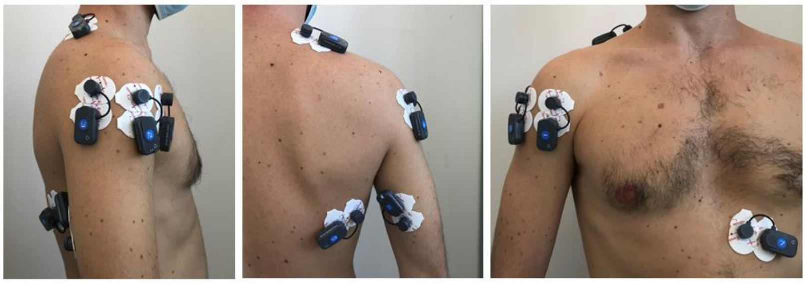

(a) (b) (c)

Figure 35: Subject 2 with the electrodes placed in the identified muscles, view from the side (a), back (b) and front (c).

5.1.4 Data recording

The EMG signals were collected using pre-gelled bipolar Ag/AgCl surface electrodes (Pirrone & Co., Milan, Italy) and acquired with a sampling frequency of 1 kHz with the BTS FREEEMG 1000 (BTS Bioengineering, Milan, Italy). The BTS software allows to store the collected data for a later offline analysis. It has to be remarked that an additional probe is placed on the exoskeleton with the intention of synchronously recording the synchronization signal generated by the exoskeleton with the EMG signals.

5.1.5 Participants

Two healthy male subjects volunteered for this study (S1: age 34 years old, height 184 cm, weight 62 kg; S2: age 28 years old, height 184 cm, weight 80 kg). The study was carried out at the premises of the BioRobotics Institute of Scuola Superiore Sant'Anna (Pontedera, Pisa, Italy). The study was approved by the local Institutional Review Board (approval n. 2/2019) and experimental activities were conducted following the principles stated in the Declaration of Helsinki. The participants signed a written informed consent. Independently on their dominant arm, both subjects were required to perform the tasks with the right hand, from the moment that the algorithm takes as input the right shoulder angle sensor signal. Figure 36 shows one of the subjects wearing the H-PULSE.

Figure 36: One of the participants (S2) wearing the H-PULSE exoskeleton.

5.1.6 Procedures

Upon arrival, the participants were informed about the study and signed the informed consent. Then, the subject familiarized with the exoskeleton and instructed on the tasks to be performed. A check for the correct wearing of the exoskeleton was done in this stage, with particular care to the straps regulation. In this step, the EMG electrodes were attached and the sensors were fixed with tapes to reduce possible movement artifacts. Before starting the tasks sequence, the MVC values were collected: the subject was asked to perform three bursts of maximum contractions lasting 5 seconds each.

In order to reduce the inter-subjects variability, the subject was placed in front of the setup structure at the right distance and the shelves were correctly regulated. Such regulations aimed at assuring that the static task is performed at around 90 degrees and, as a consequence, all the other tasks in the sequence are executed at the intended sFE angles.

Therefore, prior to the FIX-EXO trial, the fixed level of support to be provided is computed with a custom MATLAB routine and according to the biomechanical considerations reported above. For S1 the fixed support value was 3, whereas for S2 the fixed support was 4.

Once the subject was ready and the setup was regulated, the participant could start the experiment. For what concerns the sequence of actions, for each tested condition the steps were the same and can be resumed as follows. First of all, a 1-minute baseline was acquired while the subject was standing still, with the arms resting along the body in a neutral pose. Then, the participant was asked to start the tasks sequence, which had a total duration of around 6 minutes and was performed according to the movements explained above. At the end of the sequence, another baseline acquisition was performed: similar to the baseline acquisition in the beginning, the subject stood up in a resting position with the arms along the body for 1 minute.

Since only two subjects were included in this preliminary evaluation, both subjects underwent the same sequence of tasks (screwing – box handling – wall painting) and conditions (NO-EXO – AD-EXO – FIX-EXO). Between conditions, the subject had sufficient time to rest.

5.1.7 Data analysis

The data analysis was performed offline using MATLAB R2019b custom routines. The main intent of the analysis was to extract the chosen metrics from each acquired data sequence and consequently compare the three considered conditions.

Prior to the metrics calculation, the EMG linear envelope was computed for all the acquisitions. The first step involved a 4-th order band-pass Butterworth filter (cut-off frequencies: 20-400 Hz), intended to remove movement artifacts at low frequencies. Another 4-th order notch Butterworth filter (eliminating the frequencies around 50 Hz) was implemented to remove the noise disturbances coming from the power hum. Then, the signal was rectified and low-pass filtered (zero-lag 100ms moving average filter). Finally, the signal was normalized with respect to the maximum voluntary contraction (MVC), which was obtained as the maximum value from three consecutive exertions.

The EMG signal was analysed differently depending on the type of task performed. For what concerns the static case, the normalized EMG envelope of the last 30 seconds was segmented in 15 intervals of 2 seconds each. Then, the RMS value for each interval was computed and the boxplots were plotted to compare the three considered conditions. The same procedure was followed for the semi-dynamic task, whereas the dynamic task has a different process. For this kind of task, the last 15 muscle activations were manually segmented and for each of them the integral EMG (iEMG) was computed. Finally, the boxplots are plotted to analyse the behaviour in the three considered conditions.

In order to quantify the advantage of having the exoskeleton worn, the muscle activity reduction in the FIX-EXO or AD-EXO case was compared to the value obtained for the NO-EXO condition. The evaluation was made by means of a percent variation according to (5):

$$\Delta_{EMG} = \frac{exo \ - NOexo}{NOexo} \cdot 100 \quad (5)$$

It has already been demonstrated that the case with the exoskeleton worn can significantly reduce the physical strain and thus the muscles activation [4], [27], [38], [40]. Therefore, this metric is mainly aimed at investigating if there are any differences in the reduced muscles activations when using the FIX-EXO conditions with respect to the AD-EXO case, thus assessing if the adaptive or the fixed assistance can be more beneficial for the user.

In order to analyse the HR, the ECG signal was filtered to obtain the signal linear envelope, as done for the EMG signals. From the ECG signal, the R-R interval was calculated and then the HR. The main goal of the HR analysis is to highlight its changes along the time of each experimental condition. In particular, the variation between the mean HR computed before the tasks sequence and at the end of the movements was performed. This metric was used for evaluating whether the provided support can be more or less beneficial for the user over the whole execution of the tasks. In particular, similarly to the procedure adopted in a previous study on upper-limb exoskeletons [52], the cardiac cost was considered. First of all, the mean value of the HR was computed for the last 30 seconds of the baseline acquired before the starting of the movements sequence (${HR^{mean}}_{BL}$). Afterwards, the mean HR was computed for the last 30 seconds of the sequence of movements, thus at the ending of the semi-dynamic wall-painting movement (${HR^{mean}}_{work}$). Then, the variation of the mean HR of this last interval with respect to the mean value in the first baseline was computed according to (6):

$$\delta_{condition} = {HR^{mean}}_{work} - {HR^{mean}}_{BL} \quad (6)$$

Consequently, similar to the process used in the muscles' activation analysis, a percentage variation is used to quantify if the adaptive assistance can be more effective than the fixed assistance when they are compared to the condition where no exoskeleton is worn. Therefore, the variation between the NO-EXO case and the AD-EXO or FIX-EXO is computed according to (7):

$$\Delta_{HR} = \delta_{condition\ with\ exo} - \ \delta_{NO-exo} \quad (7)$$

Once the main metrics have been computed, a detailed analysis of the obtained results can highlight the main differences between the three considered conditions.

5.2 RESULTS

This chapter reports the results of the experimental trials performed in a human-in-the-loop fashion for the two volunteers of the experiment. This part is organized in two sub-chapters, each dedicated to report the results obtained for one of the subjects, with the corresponding plots and tables of the computed metrics. Firstly, the EMG envelope is plotted for the muscles' activations over the tasks sequence. Then, for each task, the boxplots and metrics are reported, whereas the last table shows the HR metrics. This chapter reports just the outcomes, whereas the following Chapter 6 is dedicated to a detailed analysis and discussion of the obtained results.

5.2.1 Subject 1

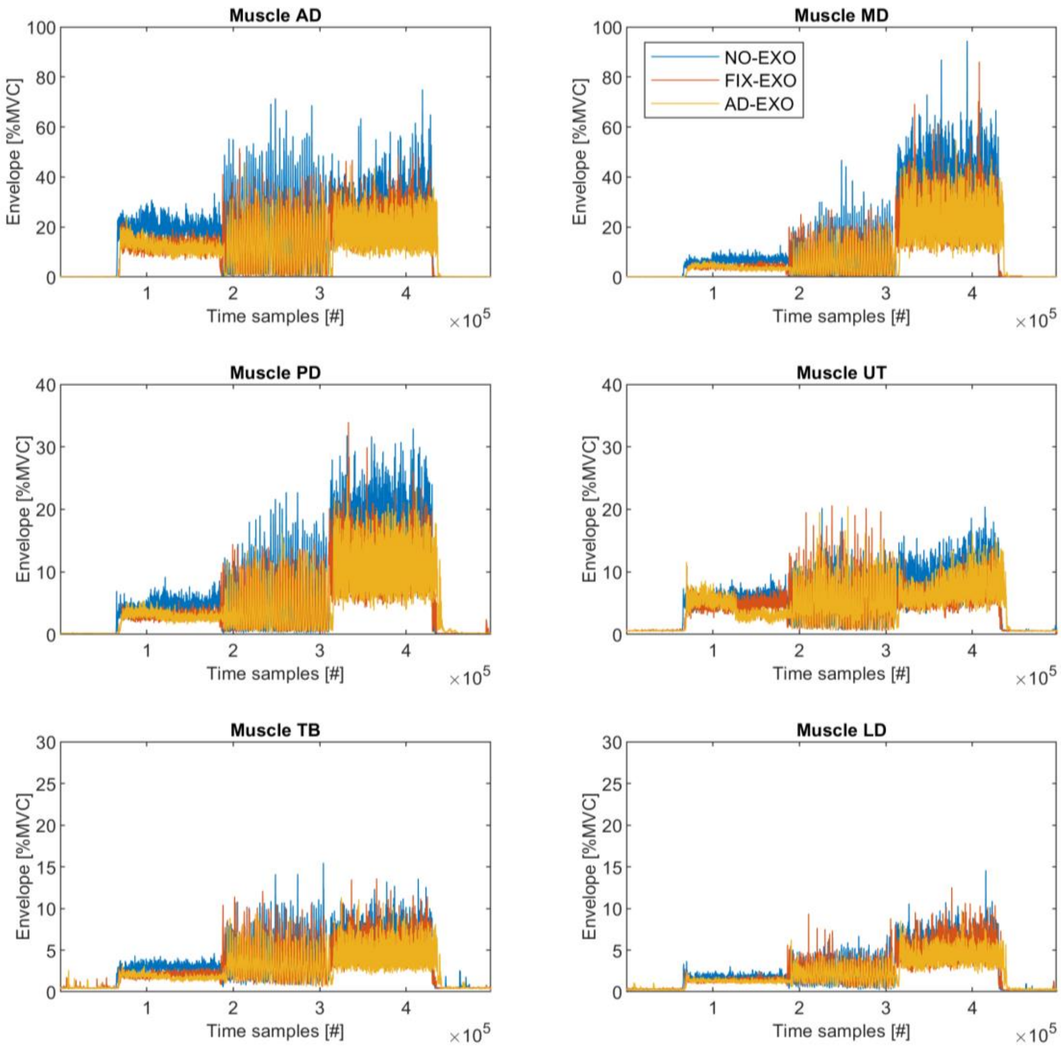

Figure 37: EMG envelope of each muscle during the experimental trials of S1.

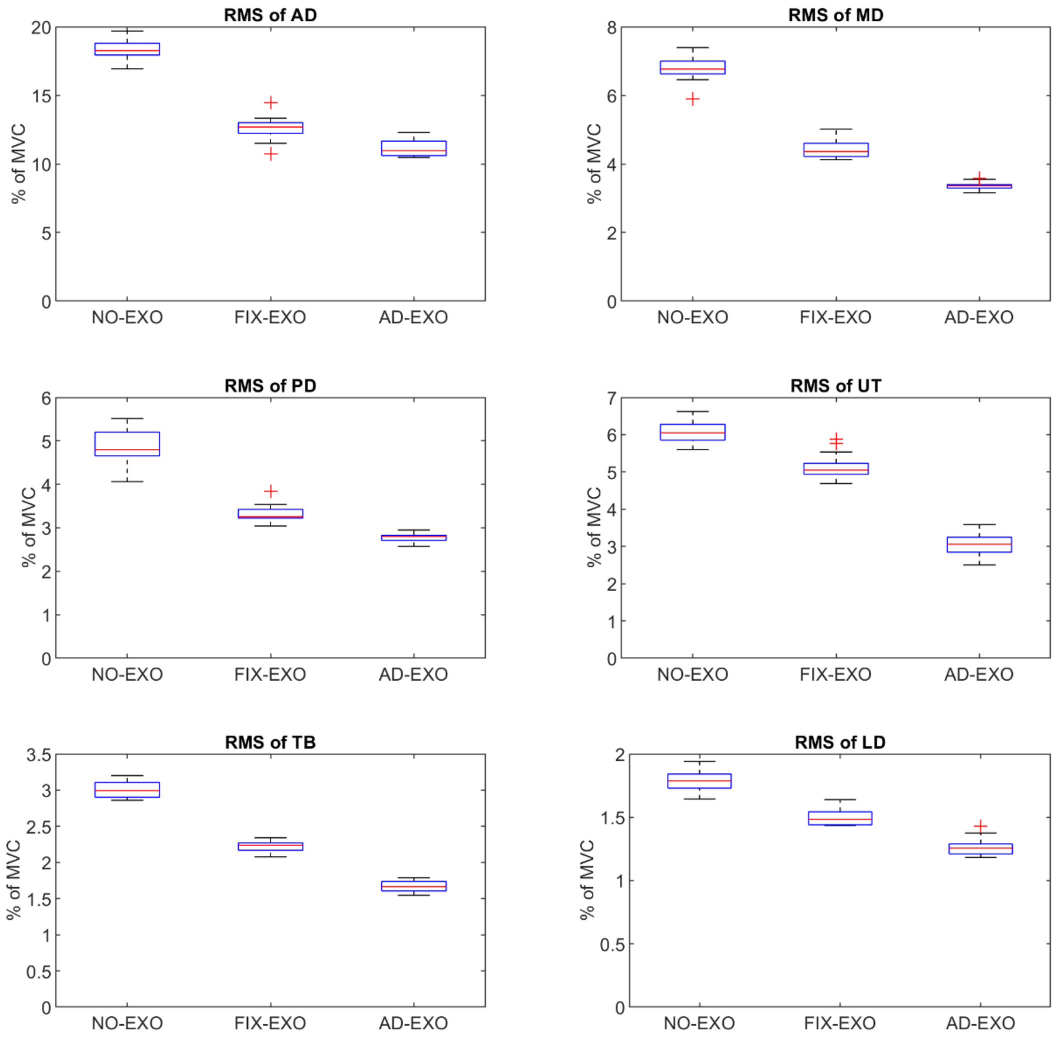

Figure 38: Boxplots of the EMG RMS distribution over the last 30s of the screwing static task – S1.

Muscle	Δ_{EMG} ***FIX-EXO***	Δ_{EMG} ***AD-EXO***
AD	–32.4 %	–40.2 %
MD	–35.6 %	–51.1 %
PD	–32.2 %	–43.7 %
UT	–15.1 %	–49.9 %
TB	–26.7 %	–45.0 %
LD	–17.5 %	–30.2 %

Table 3: EMG RMS reduction in the FIX-AD and AD-EXO cases with respect to the NO-EXO case – S1.

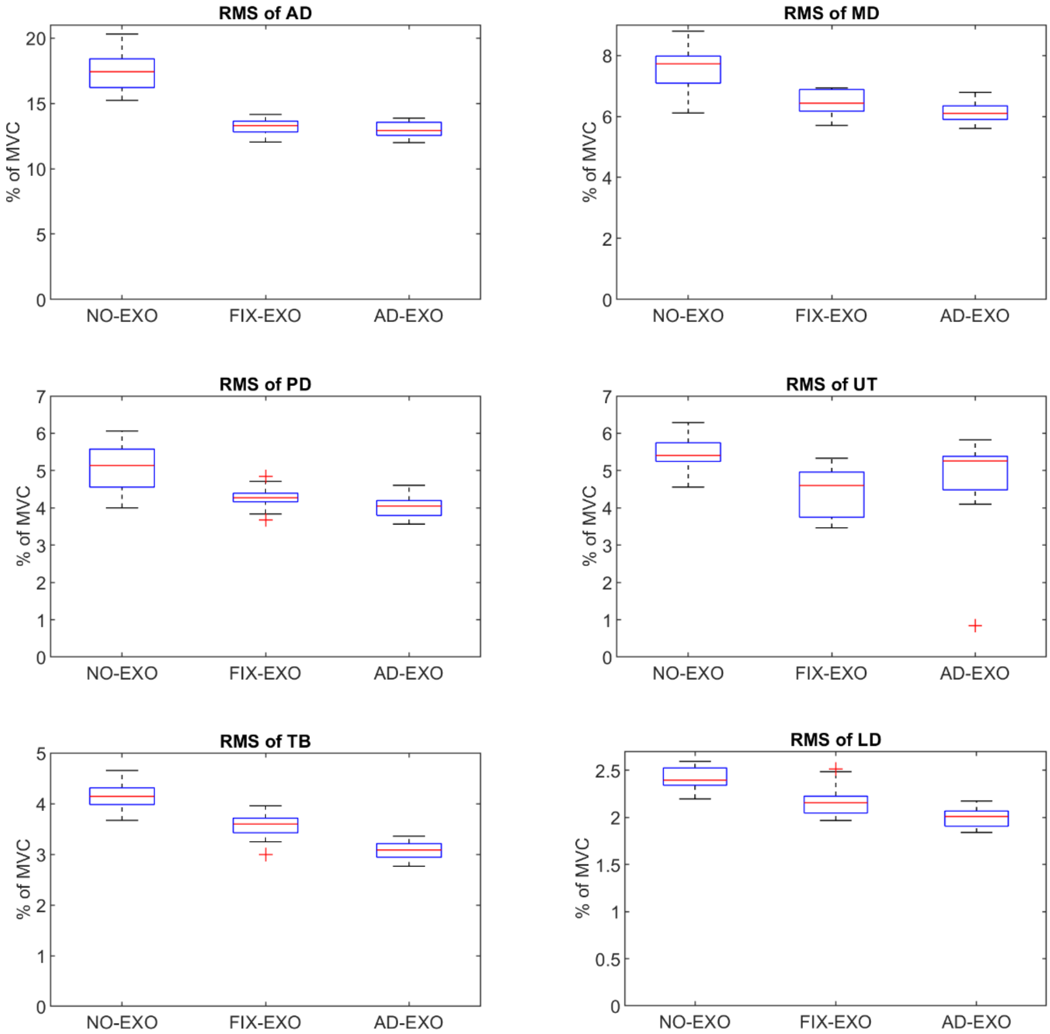

Figure 39: Boxplots of the iEMG distribution over the last 15 muscle activations of the box handling dynamic task – S1.

Muscle	Δ_{EMG} ***FIX-EXO***	Δ_{EMG} ***AD-EXO***
AD	– 24.0 %	– 25.3 %
MD	– 15.2 %	– 19.6 %
PD	– 15.6 %	– 20.3 %
UT	– 17.9 %	– 12.3 %
TB	– 14.5 %	– 25.8 %
LD	– 10.2 %	– 16.9 %

Table 4: iEMG reduction in the FIX-AD and AD-EXO cases with respect to the NO-EXO case – S1.

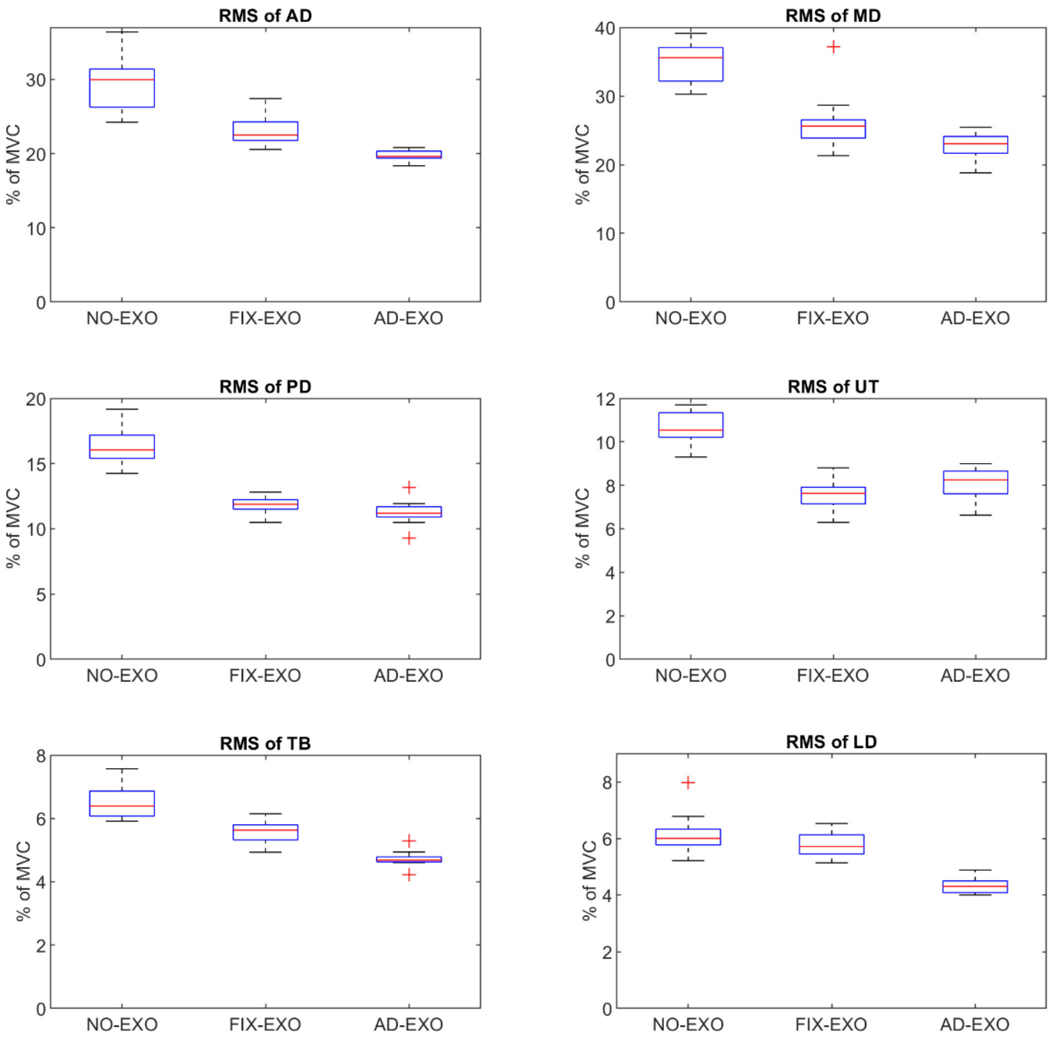

Figure 40: Boxplots of the EMG RMS distribution over the last 30s of the wall painting semi-dynamic task – S1.

Muscle	Δ_{EMG} ***FIX-EXO***	Δ_{EMG} ***AD-EXO***
AD	– 21.8 %	– 32.8 %
MD	– 26.3 %	– 34.7 %
PD	– 27.8 %	– 31.3 %
UT	– 29.1 %	– 23.9 %
TB	– 14.4 %	– 27.3 %
LD	– 5.8 %	– 29.6 %

Table 5: EMG RMS reduction in the FIX-AD and AD-EXO cases with respect to the NO-EXO case – S1.

Condition	δ_{HR}	Δ_{HR}
NO-EXO	+ 25 bpm	/
FIX-EXO	+ 14 bpm	–11 bpm
AD-EXO	+ 20 bpm	–5 bpm

Table 6: HR metrics of S1.

5.2.2 Subject 2

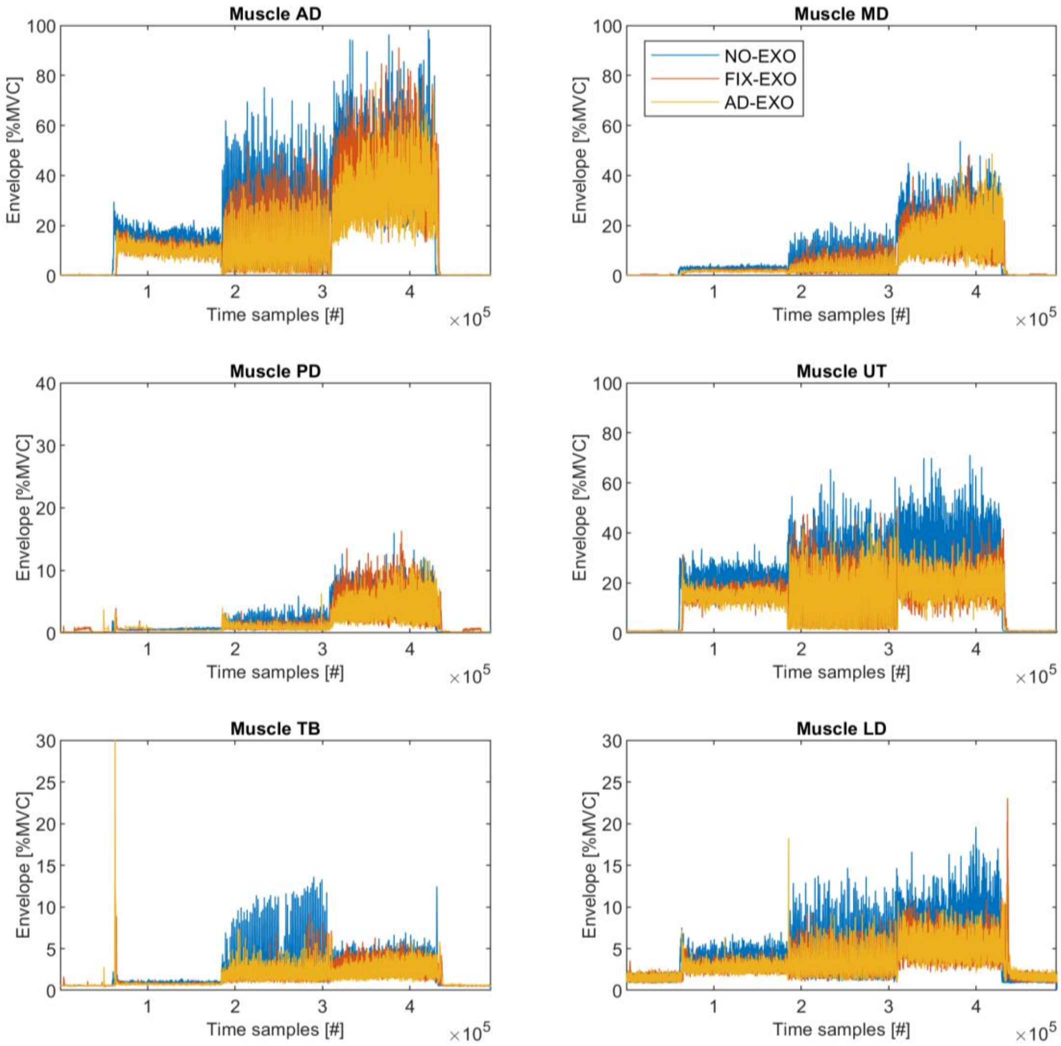

Figure 41: EMG envelope of each muscle during the experimental trials of S2.

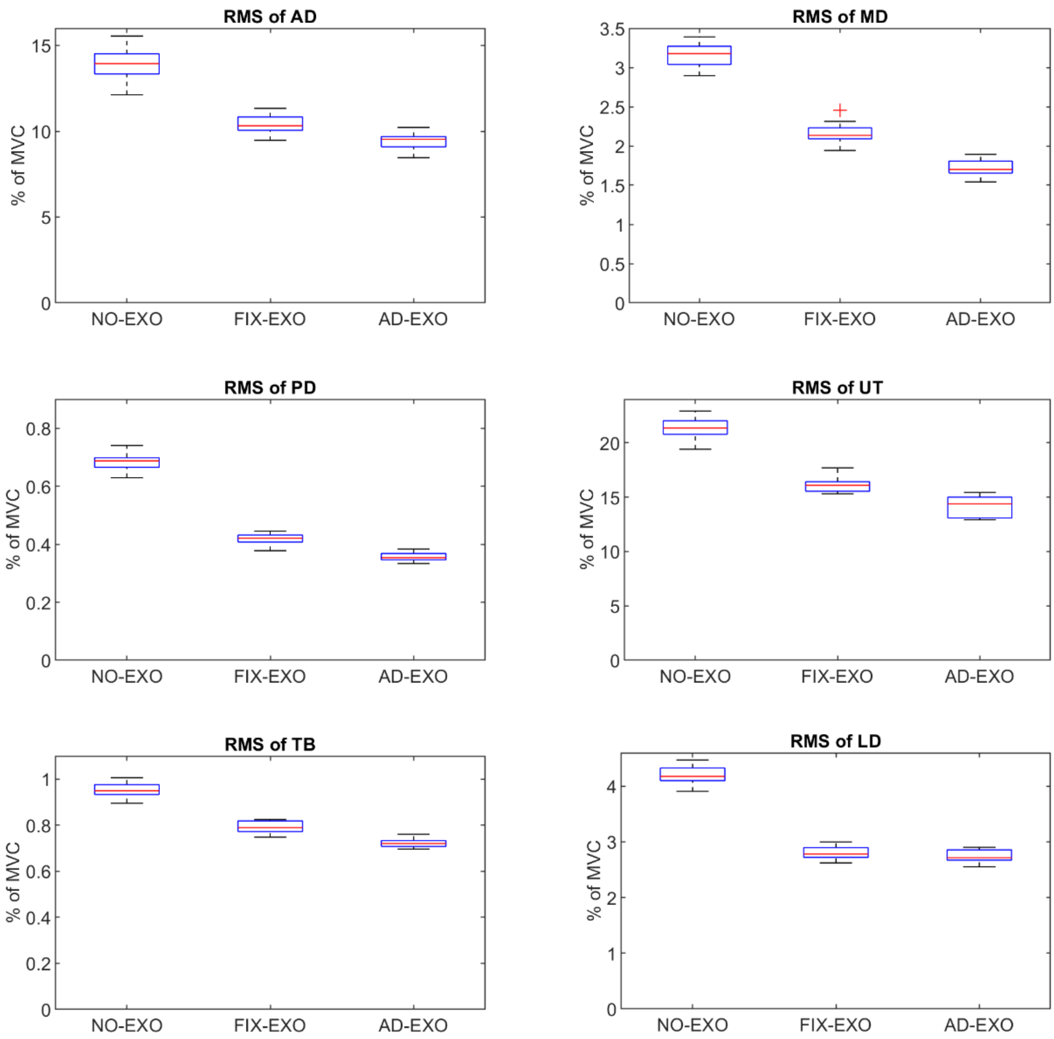

Figure 42: Boxplots of the EMG RMS distribution over the last 30s of the screwing static task – S2.

Muscle	Δ_{EMG} ***FIX-EXO***	Δ_{EMG} ***AD-EXO***
AD	–25.1 %	–32.3 %
MD	–31.6 %	–45.5 %
PD	–38.8 %	–47.6 %
UT	–24.5 %	–33.5 %
TB	–16.9 %	–24.1 %
LD	–33.1 %	–34.6 %

Table 7: EMG RMS reduction in the FIX-AD and AD-EXO cases with respect to the NO-EXO case – S2.

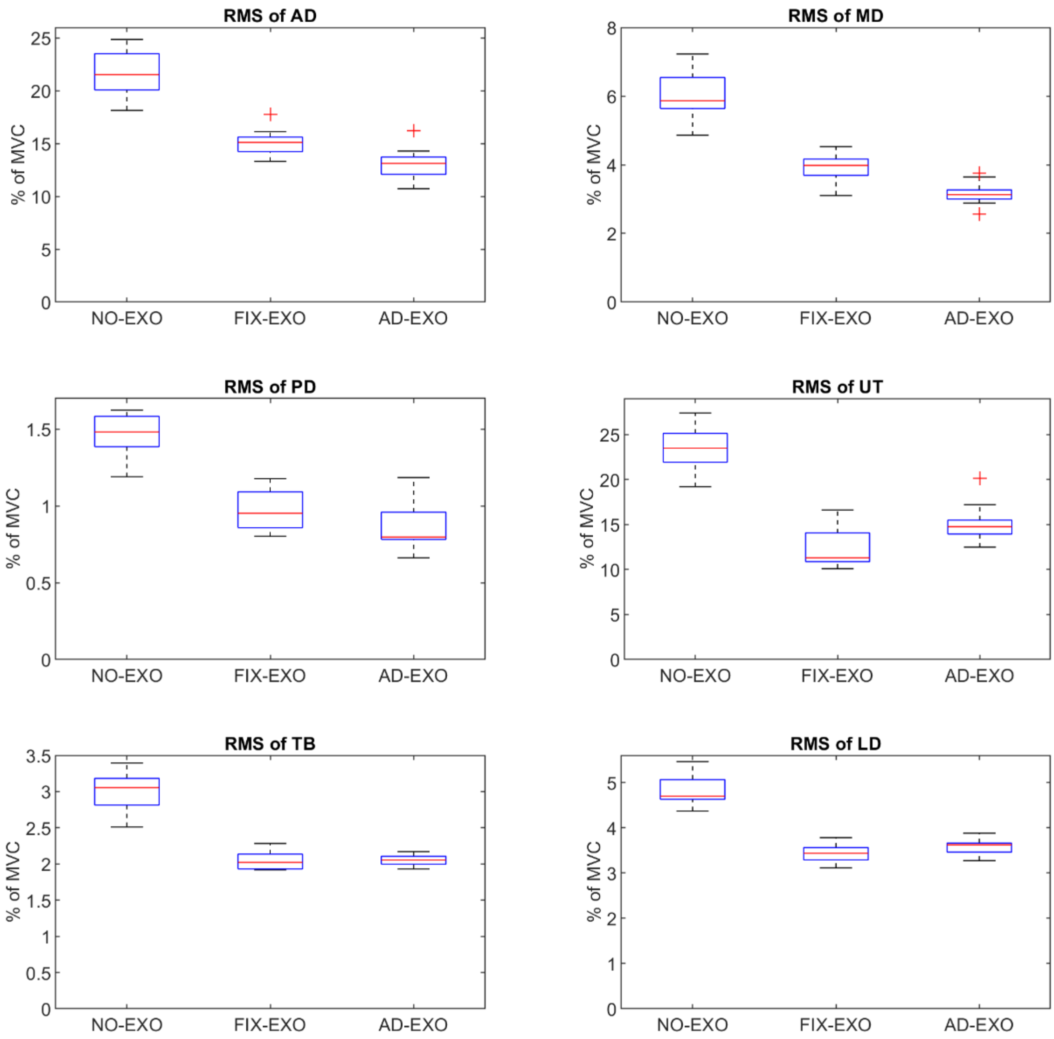

Figure 43: Boxplots of the iEMG distribution over the last 15 muscle activations of the box handling dynamic task – S2.

Muscle	Δ_{EMG} ***FIX-EXO***	Δ_{EMG} ***AD-EXO***
AD	– 30.5 %	– 39.9 %
MD	– 35.5 %	– 47.4 %
PD	– 34.5 %	– 41.4 %
UT	– 47.9 %	– 35.9 %
TB	– 31.7 %	– 31.5 %
LD	– 28.0 %	– 25.3 %

Table 8: iEMG reduction in the FIX-AD and AD-EXO cases with respect to the NO-EXO case – S2.

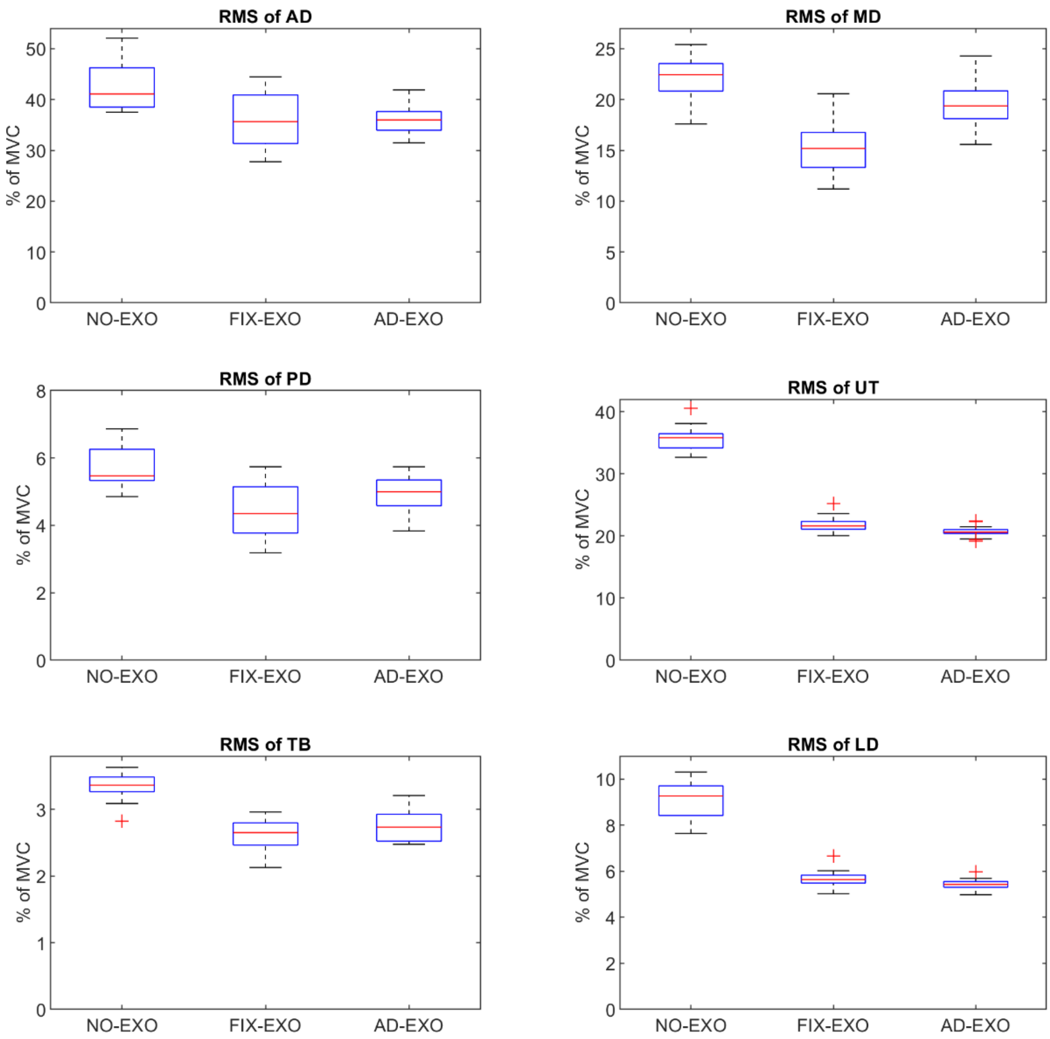

Figure 44: Boxplots of the EMG RMS distribution over the last 30s of the wall painting semi-dynamic task – S2.

Muscle	Δ_{EMG} ***FIX-EXO***	Δ_{EMG} ***AD-EXO***
AD	– 14.4 %	– 14.9 %
MD	– 31.0 %	– 12.4 %
PD	– 22.5 %	– 14.1 %
UT	– 38.5 %	– 41.9 %
TB	– 22.4 %	– 18.4 %
LD	– 37.3 %	– 40.1 %

Table 9: EMG RMS reduction in the FIX-AD and AD-EXO cases with respect to the NO-EXO case – S2.

Condition	$\boldsymbol{\delta_{HR}}$	$\boldsymbol{\Delta_{HR}}$
NO-EXO	+ 8 bpm	/
FIX-EXO	+ 9 bpm	+ 1 bpm
AD-EXO	+ 0 bpm	–3 bpm

Table 10: HR metrics of S2.

6 DISCUSSION

In the previous chapters, the algorithm development and the human-in-the-loop experimental activities have been described in details. This chapter is instead dedicated to the investigation and discussion of the results (reported in Chapter 5) obtained during the experimental validation of the adaptive algorithm.

In line with previous studies [4], [27], [38], [40], for both subjects and in all the executed tasks, the conditions with the exoskeleton worn showed significant reductions in the muscles activation with respect to the condition where no device is worn, thus confirming that the supportive action can be potentially beneficial to prevent muscle strain and fatigue. However, a more detailed analysis must be carried out to analyse the benefits coming from an adaptive assistance with respect to the case where a fixed level of support is provided.

This section is divided in two sub-sections in a similar fashion with respect to the previous one. Indeed, each subject has a dedicated sub-chapter with the analysis of the results obtained for its experimental trials.

6.1.1 Subject 1

Subject 1 showed an overall reduction in the muscles activation when the exoskeleton is worn with respect to the condition without the exoskeleton in all the considered tasks (Figure 37). Starting from the static task, the boxplots and percentage metrics (Figure 38 and Table 3) highlight how the exoskeleton use can significantly reduce the muscles activations. A significant example resides in the AD, where in the FIX-EXO condition the reduction is -32.4 % and in the AD-EXO case the reduction reaches -40.2%. A similar trend is highlighted for the MD and UT, the muscles that with the AD represent the main agonist muscles during the flexion-extension of the arm. These three muscles have the highest reductions in the activations when performing the static task. This result is in line with the study conducted on the Proto-MATE [27], where it was highlighted how the reduction in the EMG activation of agonist muscles lead to a reduced muscles strain. In particular, the UT decreased activity can have important benefits for the back/spine as well. Indeed, a previous study suggested that the reduced UT activation might imply a smaller spinal loading, since this muscle is the main actor when transferring the loads from the shoulders to the back and the hip belt [22].

An important comparison involves the FIX-EXO and the AD-EXO conditions (Table 3). During the static task execution, all muscles for S1 showed a greater reduction with respect to the NO-EXO case when the support level was chosen according to the adaptive algorithm. This behaviour is justified by the fact that the fixed support level for S1 is set to 3, whereas the adaptive algorithm during the execution of the static task reaches the support level of 6. This result, first of all, confirms the hypothesis used for the algorithm design and suggested by some previous studies [28], [40] that a greater support might be needed in case of static prolonged tasks. Moreover, it highlights the benefits of the support level chosen according to an adaptive algorithm over a pre-fixed support, since the algorithm can better adapt to the system behaviour.

Moving into the second task, namely the box handling movements, other considerations arise from the performed analysis (Figure 39 and Table 4). Globally, the conditions with the exoskeleton once again proved to be beneficial with respect to the NO-EXO condition, since the EMG activations were reduced for all muscles when the device was worn. This result is of paramount importance when considering dynamic tasks, since one of the main goal when wearing an exoskeleton is to avoid the activation of antagonist muscles, thus avoiding that the exoskeleton hinders the movements and obstructs the user during the task execution [22].

Considering a detailed comparison between the FIX-EXO and the AD-EXO conditions, smaller differences between the two cases were highlighted when performing the dynamic task (Table 4). As a matter of facts, these two conditions have similar results in the decrease of the muscles activations when compared to the NO-EXO case. This result may be in contrast with respect to the different support levels provided by the two conditions, namely 3 for the fixed case and 0 from the adaptive algorithm condition. However, a deeper investigation remarks that a significant difference is found for the TB and LD muscles, which have a greater reduction in the adaptive assistance case (-25.8% and -16.9% in contrast to -14.5% and -10.2 % for the FIX-EXO case). This can yield to interesting conclusions, since these two muscles are the two main actors when performing dynamic movements, as they act as antagonist muscles during shoulder flexion-extension. Therefore, as previously suggested, it is of great importance to find a correct balance between agonist and antagonist muscle activations when wearing an exoskeleton [40], otherwise an unwanted increased activation of antagonist muscles can happen [22]. Indeed, the adaptive assistance level in this case becomes more effective in reducing the activation of these muscles during the dynamic task movements.

Moving into the last task of the sequence, during the semi-dynamic task both conditions with the exoskeleton worn showed significant muscles activations reductions with respect to the case where no exoskeleton is worn (Figure 40 and Table 5). This movement is introduced in the sequence to investigate if the device can be effective also in a case where no strict distinction between static and dynamic movement can be made. A previous study already highlighted how exoskeleton can be equally applied to static and dynamic tasks [22], therefore this experimental trial confirms the benefits of using the device also for other hybrid types of movements.

When analysing the semi-dynamic task, some important differences are highlighted in the muscles' activity reduction for the fixed assistance case and the adaptive assistance with respect to the case of NO-EXO (Table 5). It should be noted that the support level provided by the adaptive algorithm for S1 was 3 for this last task, which is the same value as the fixed level pre-set for S1. This could suggest that the expected results are similar in terms of muscles activations reductions. However, this is not the case, since some differences are present from the AD-EXO conditions with respect to the FIX-EXO case. To explain this trend, the whole sequence of actions should be observed. Indeed, these discrepancies might be linked to the fact that in the FIX-EXO condition the fixed assistance level remains the same for the whole duration of the movements sequence, whereas the AD-EXO case has a support level that changes dynamically in real time and assumes different values over the whole sequence. Therefore, being the semi-dynamic task the last of the sequence, the muscles could be affected by how much the assistance of the previous static and dynamic tasks helped in reducing the overall strain and fatigue.

Focusing on the main differences, the AD-EXO case is more effective in reducing the activation of TB and LD case (-27.3% and -29.6% in contrast to -14.4% and -5.8 % for the FIX-EXO case). This leads to the conclusion that the antagonist muscles can have reduced activations with the adaptive support. On the other hand, the UT shows greater reductions in the FIX-EXO case, suggesting that this condition is slightly less demanding for this muscle and, as previously mentioned, for the back and spine.

Finally, for what concerns the cardiac cost, the case where the exoskeleton is worn shows a smaller increase in the HR value at the end of the tasks sequence (Table 6). This is an encouraging result, since wearing an exoskeleton could imply a greater cardiac cost coming from the additional weight that the user has to carry [52]. However, this is not the case, and the reason may reside in the muscles overall reduced activations with respect to the NO-EXO case, thus in a smaller overall fatigue for the user.

Overall, the trial with S1 highlights some important benefits in terms of reduced muscles activations and overall fatigue, demonstrating how the adaptive algorithm can be in general more effective than a fixed level of assistance when diversified tasks are executed.

6.1.2 Subject 2

Subject 1 is of paramount importance for the proof of concept and efficacy assessment of the adaptive support provided by H-PULSE. However, in order to see if the results hold also for other volunteers, subject 2 represents an important confirmation of the obtained results (Figure 41).

Starting from the static task, the boxplots and percentage metrics (Figure 42 and Table 7) show how the exoskeleton worn can significantly reduce the muscles activations. The deltoids are the muscle complex that benefits the most from having the support provided by the exoskeleton. In fact, muscle activity reductions for the PD are up to -38.8 % for the FIX-EXO case and -47.6 % in the AD-EXO case. Similar results hold for AD and MD, showing a similar trend in S2 with respect to S1. This reduced activation for the deltoid muscles highlights the helpful action of the exoskeleton in preventing the insurgence of rotator cuff injuries, as suggested in another study on the biomechanical effectiveness of industrial exoskeletons [29].

Moreover, similarly to S1, also S2 has a greater muscle activity reduction in the case where the adaptive assistance is set in real time (Table 7). This confirms that the greater support provided in the AD-EXO case (reaching the level of 6), is more helpful in reducing the physical muscle fatigue with respect to the FIX-EXO case, where the assistance remains fixed at level 4. Moreover, the hypothesis to provide more support in case of static movements is confirmed to be an effective implementation and thus it confirms the effectiveness of the adaptive assistance for this kind of tasks. This result also reflects the conclusions of previous studies where different assistance levels were selected for passive exoskeletons. Indeed, the ShoulderX device showed greater reduction in muscles activations with increasing assistive peak torque [24] and a previous study on the H-PULSE showed reduced activations when a greater level of assistance was provided [36].

Moving into the dynamic tasks, some important considerations arise for S2 (Figure 43 and Table 8). Once again, the exoskeleton worn significantly helps in reducing the muscles activation. A relevant example is represented by the MD, having reductions up to -35.5 % in the FIX-EXO case and -47.4% in the AD-EXO conditions. Likewise, antagonist muscles (mostly TB and LD) show decreased activations in both conditions with the exoskeleton worn, which is an important aspect when avoiding antagonist muscles activations during dynamic movements [22].

During the dynamic task, when comparing the FIX-EXO with the AD-EXO condition, the overall trend shows grater muscle reduction for the adaptive case (Table 8). This is in line with the results obtained for S1, confirming that a smaller support is beneficial during dynamic tasks. In fact, the adaptive algorithm reaches a level 0 of support during the execution of this task, whereas the fixed level for S2 is 4. The only exception is represented by the UT muscle, which shows a greater reduction in the FIX-EXO case. This point must not be ignored, since the UT muscle is fundamental to stabilize the whole upper trunk region of the body [29], so further investigations will be performed to analyse more in depth how much this greater reduced activation can benefit the user over longer periods.

The last semi-dynamic task shows a similar trend in the reduction of muscle activity, always highlighting the beneficial effect of having the exoskeleton worn with respect to the condition of NO-EXO, confirming the promising results of the exoskeleton support highlighted for S1 (Figure 44 and Table 9). However, when comparing the FIX-EXO with the AD-EXO, some interesting behaviours arise (Table 9). Globally, muscles show a similar percentage reduction with respect to the NO-EXO case. However, MD and PD have higher reduction in the fixed assistance case. To understand this behaviour, a comparison between levels of support must be made. In fact, for S2 the given support level is the pre-set value of 4. On the other hand, the adaptive algorithm reaches the level of support of 2, which is lower than the level reached for S1. This behaviour is related to the pacing of the movements, which was not imposed to the subjects to reflect a working condition where the worker can choose its own pace. It was remarked that S2 performed the movements with a faster pace with respect to S1 and the algorithm could only reach the assistance value of 2. This suggests that the algorithm did not reach the steady state after the two minutes of the trials, therefore the given support was not sufficient to be more beneficial to the user than the fixed case. Further investigations are needed to highlight this variability between the chosen movement strategy.

Finally, some important remarks are highlighted for S2 concerning the HR variations (Table 10). The cardiac cost for S2 is reduced when wearing the exoskeleton in the adaptive case, whereas no significant difference is remarked in the FIX-EXO condition with respect to the NO-EXO case. This slight improvement for the adaptive condition is promising to assess the effectiveness of the adaptive strategy. Indeed, it is of paramount importance to consider how the physiological demand can change when performing difficult tasks and how the exoskeleton can affect this physiological parameter [52].

Overall, S2 shows interesting results that are aligned with the ones obtained for S1, thus confirming the promising results obtained in terms of reduced fatigue and strain when exploiting ad adaptive assistance strategy. Further investigations are still needed to completely assess the adaptive assistance efficacy, implying for instance a wider number of subjects or larger and more informative metrics.

7 CONCLUSION

This thesis work presented the development and experimental validation of a novel adaptive control for the online computation of the assistance given by the semi-passive exoskeleton H-PULSE. The main goal during the design phase was to exploit the shoulder kinematics in order to compute the desired level of support. Subsequently, experimental activities were carried out to have a preliminary efficacy assessment of the adaptive algorithm when it is implemented in the real-time controller of the exoskeleton. Indeed, the main objectives of the experimental trials were the investigation of the effects of the adaptive control strategy against experimental conditions where the exoskeleton was not worn (i.e. without any support) or delivered a fixed and predetermined level of assistance (i.e. supporting about the 50% of the arm gravitational torque).

Firstly, the design phase successfully managed to linearly combine the extracted kinematic features. The result was a finite different equation formulation that could accurately follow the evolution of the system and dynamically change the support level in real time. The algorithm behaved as intended, with an increase of the support during more demanding tasks, namely more static actions and movements at elevations angles of about 90 degrees. On the other hand, the support level decreased when the user's actions did not have to be hindered, namely during more dynamic tasks or movements around very high and very low elevation angles. Once the desired algorithm behaviour was achieved, the real time implementation followed.

The algorithm was implemented online in the exoskeleton controller and the efficacy of the chosen adaptive strategy was assessed by means of experimental trials. The experimental trials aimed at extracting relevant metrics to quantify the muscle strain and the physiological demand in terms of changes in the heart rate. Therefore, EMG signals were acquired and elaborated to extract relevant information for each of the three considered conditions (no exoskeleton worn against a fixed or adaptive assistance from the device).

The results of the experimental trials highlighted how the device worn could significantly reduce the muscle fatigue of the main shoulder muscles and decrease the heart rate cardiac cost over the sequence of movements. Moreover, when the device was worn with the adaptive control, the result was a globally reduced muscle activation and cardiac cost in the performed tasks with respect to the case where the assistance was fixed. In particular, during static movements, the adaptive strategy managed to reduce up to -40% the activation of the deltoids. In case of more dynamic movements, the activation of antagonist muscles, except the upper trapezius, where significantly reduced in both subjects when the movement was assisted by the adaptive assistance. Lastly, semi-dynamic tasks showed promising results in the first subject, with a generally lower muscles activation, whereas subject 2 did not show such a relevant difference with respect to the fixed assistance case. Lastly, the heart rate cardiac cost was significantly reduced in subject 2 when the support level was chosen according to the adaptive strategy. This suggested that the overall physiological demand could be decreased when using an adaptive control strategy.

Although the obtained results are promising, some limitations can be remarked. First of all, the number of subjects was limited and no statistical analysis could be performed. However, the two subjects were fundamental for the preliminary efficacy assessment of the adaptive algorithm. Secondly, the sequence of tasks was limited to just three types of movements, therefore it did not explore other possible work-inspired actions. Lastly, the adaptive control strategy managed to reduce muscles activations in most of the considered muscles, however some muscles still showed more benefits in the fixed assistance case.

Following these limitations, additional work still needs to be done to overcome the highlighted flaws. First of all, a higher number of subjects can be recruited in order to analyse more deeply the advantages of the adaptive control and perform a statistical analysis on the results. Consequently, the number of tasks can be augmented to consider more diversified working conditions and study if the exoskeleton can be beneficial also with different types of movements. In conclusion, a deeper analysis of the muscles' activations with the use of other structured metrics could lead to a more detailed study on the muscles' activation and strain during the performed movements.

8 BIBLIOGRAPHY

[1] European Agency for Safety and Health at Work, “Introduction to work - related musculoskeletal disorders,” *Eur. Agency Saf. Heal. Work*, vol. 1681, no. 2123, pp. 4–8, 2007, [Online]. Available: https://osha.europa.eu/sites/default/files/publications/documents/en/publications/factsheets/71/Factsheet_71_-_Introduction_to_work-related_musculoskeletal_disorders.pdf.

[2] J. De Kok *et al.*, “Work-related MSDs: prevalence, costs and demographics in the EU (European Risk Observatory Executive summary),” *Publ. Off. Eur. Union*, pp. 1–18, 2019.

[3] B. Hartmann, *Work-related musculoskeletal disorders*, vol. 60, no. 11. 2010.

[4] P. Maurice *et al.*, “Objective and Subjective Effects of a Passive Exoskeleton on Overhead Work,” *IEEE Trans. Neural Syst. Rehabil. Eng.*, vol. 28, no. 1, pp. 152–164, 2020, doi: 10.1109/TNSRE.2019.2945368.

[5] D. Romero *et al.*, “Towards an operator 4.0 typology: A human-centric perspective on the fourth industrial revolution technologies,” *CIE 2016 46th Int. Conf. Comput. Ind. Eng.*, no. October, pp. 0–11, 2016.

[6] B. P. Bernard, “Musculoskeletal Disorders and Workplace Factors,” *A Crit. Rev. Epidemiol. Evid. Work. Musculoskelet. Disord. Neck, Up. Extrem. Low Back*, no. February 2015, 1997.

[7] B. Eovaldi and M. Varacallo, “Anatomy, Shoulder and Upper Limb, Shoulder,” *StatPearls*, no. December, 2018, [Online]. Available: http://www.ncbi.nlm.nih.gov/pubmed/30725618.

[8] E. Levangie, Pamela and Cynthia C. Norkin, *Joint Structure and Function: A Comprehensive Analysis. 5th ed.* 2011.

[9] L. Keswick, “Breast Anatomy - Medical Art Library.” https://medicalartlibrary.com/shoulder-anatomy/ (accessed Oct. 07, 2021).

[10] K. Ohlsson *et al.*, “Repetitive industrial work and neck and upper limb disorders in females.,” *Am. J. Ind. Med.*, vol. 27, no. 5, pp. 731–747, May 1995, doi: 10.1002/ajim.4700270508.

[11] B. Stenlund, I. Goldie, M. Hagberg, and C. Hogstedt, “Shoulder tendinitis and its relation to heavy manual work and exposure to vibration.,” *Scand. J. Work. Environ. Health*, vol. 19, no. 1, pp. 43–49, Feb. 1993, doi: 10.5271/sjweh.1505.

[12] S. W. Svendsen, J. P. Bonde, S. E. Mathiassen, K. Stengaard-Pedersen, and L. H. Frich, “Work related shoulder disorders: Quantitative exposure-response relations with reference to arm posture,” *Occup. Environ. Med.*, vol. 61, no. 10, pp. 844–853, 2004, doi: 10.1136/oem.2003.010637.

[13] Eurofound, “Managing musculoskeletal disorders,” no. July, pp. 1–120, 2015, [Online]. Available: https://www.eurofound.europa.eu/observatories/eurwork/comparative-information/managing-musculoskeletal-disorders.

[14] J. R. Wilson, “Ergonomics and participation,” *Eval. Hum. Work A Pract. Ergon. Methodol.*, vol. 2, pp. 1071–1096, 1995.

[15] R. Burgess-Limerick, “Participatory ergonomics: Evidence and implementation lessons,” *Appl. Ergon.*, vol. 68, no. August 2017, pp. 289–293, 2018, doi: 10.1016/j.apergo.2017.12.009.

[16] R. Kadefors, T. Engström, J. Petzäll, and L. Sundström, “Ergonomics in parallelized car assembly: A case study, with reference also to productivity aspects,” *Appl. Ergon.*, vol. 27, no. 2, pp. 101–110, 1996, doi: 10.1016/0003-6870(95)00064-X.

[17] N. Sylla, V. Bonnet, F. Colledani, and P. Fraisse, “Ergonomic contribution of ABLE exoskeleton in automotive industry,” *Int. J. Ind. Ergon.*, vol. 44, no. 4, pp. 475–481, 2014, doi: 10.1016/j.ergon.2014.03.008.

[18] A. Roby-Brami and N. Jarrassé, “Wearable robotic systems and their applications for neurorehabilitation,” *Rehabil. Robot.*, no. January 2019, pp. 241–252, 2018, doi: 10.1016/b978-0-12-811995-2.00019-9.

[19] S. K. Banala, S. K. Agrawal, and J. P. Scholz, “Active Leg Exoskeleton (ALEX) for gait rehabilitation of motor-impaired patients,” *2007 IEEE 10th Int. Conf. Rehabil. Robot. ICORR’07*, vol. 00, no. c, pp. 401–407, 2007, doi: 10.1109/ICORR.2007.4428456.

[20] A. Chu, H. Kazerooni, and A. Zoss, “On the biomimetic design of the Berkeley Lower Extremity Exoskeleton (BLEEX),” in *Proceedings - IEEE International Conference on Robotics and Automation*, 2005, vol. 2005, pp. 4345–4352, doi: 10.1109/ROBOT.2005.1570789.

[21] J. L. Pons, *Wearable Robots*. Chichester, UK: John Wiley & Sons, Ltd, 2008.

[22] L. Van Engelhoven, N. Poon, H. Kazerooni, A. Ban, D. Rempel, and C. Harris-Adamson,

"Evaluation of an adjustable support shoulder exoskeleton on static and dynamic Overhead tasks," *Proc. Hum. Factors Ergon. Soc.*, vol. 2, pp. 804–808, 2018, doi: 10.1177/1541931218621184.

[23] A. Moyon, J. Petiot, and E. Poirson, "Investigating the effects of passive exoskeletons and familiarization protocols on arms-elevated tasks," *Hum. Factors Ergon. Soc. Eur. Chapter 2019 Annu. Conf.*, no. July 2020, pp. 1–17, 2019.

[24] L. Van Engelhoven and H. Kazerooni, "Design and Intended Use of a Passive Actuation Strategy for a Shoulder Supporting Exoskeleton," *2019 Wearable Robot. Assoc. Conf. WearRAcon 2019*, pp. 7–12, 2019, doi: 10.1109/WEARRACON.2019.8719402.

[25] M. P. de Looze, T. Bosch, F. Krause, K. S. Stadler, and L. W. O'Sullivan, "Exoskeletons for industrial application and their potential effects on physical work load," *Ergonomics*, vol. 59, no. 5, pp. 671–681, 2016, doi: 10.1080/00140139.2015.1081988.

[26] S. Spada, L. Ghibaudo, S. Gilotta, L. Gastaldi, and M. P. Cavatorta, "Investigation into the Applicability of a Passive Upper-limb Exoskeleton in Automotive Industry," *Procedia Manuf.*, vol. 11, no. June, pp. 1255–1262, 2017, doi: 10.1016/j.promfg.2017.07.252.

[27] I. Pacifico *et al.*, "An experimental evaluation of the proto-mate: A novel ergonomic upper-limb exoskeleton to reduce workers' physical strain," *IEEE Robot. Autom. Mag.*, vol. 27, no. 1, pp. 54–65, 2020, doi: 10.1109/MRA.2019.2954105.

[28] K. Huysamen, T. Bosch, M. de Looze, K. S. Stadler, E. Graf, and L. W. O'Sullivan, "Evaluation of a passive exoskeleton for static upper limb activities," *Appl. Ergon.*, vol. 70, no. August 2017, pp. 148–155, 2018, doi: 10.1016/j.apergo.2018.02.009.

[29] T. Schmalz *et al.*, "Biomechanical and metabolic effectiveness of an industrial exoskeleton for overhead work," *Int. J. Environ. Res. Public Health*, vol. 16, no. 23, 2019, doi: 10.3390/ijerph16234792.

[30] T. Butler and J. C. Gillette, "Exoskeletons used as PPE for Injury Prevention," *Prof. Saf.*, vol. 64, no. 3, pp. 33–37, 2019, [Online]. Available: https://lib.dr.iastate.edu/kin_pubs/47.

[31] B. Marinov, "Passive Exoskeletons Establish A Foothold In Automotive Manufacturing," *Forbes*, 2018. https://headtopics.com/us/passive-exoskeletons-establish-a-foothold-in-automotive-manufacturing-5895448 (accessed Sep. 25, 2021).

[32] P. de Leva, "Adjustments to Zatsiorsky-Seluyanov's segment inertia parameters," *J.*

Biomech., vol. 29, no. 9, pp. 1223–1230, 1996, doi: https://doi.org/10.1016/0021-9290(95)00178-6.

[33] C. Lauretti *et al.*, “Learning by demonstration for motion planning of upper-limb exoskeletons,” *Front. Neurorobot.*, vol. 12, no. FEB, pp. 1–14, 2018, doi: 10.3389/fnbot.2018.00005.

[34] Y. M. Zhou, C. Hohimer, T. Proietti, C. T. O’Neill, and C. J. Walsh, “Kinematics-based Control of an Inflatable Soft Wearable Robot for Assisting the Shoulder of Industrial Workers,” *IEEE Robot. Autom. Lett.*, vol. 3766, no. c, pp. 1–8, 2021, doi: 10.1109/LRA.2021.3061365.

[35] A. Ebrahimi, “Stuttgart Exo-Jacket: An exoskeleton for industrial upper body applications,” *Proc. - 2017 10th Int. Conf. Hum. Syst. Interact. HSI 2017*, pp. 258–263, 2017, doi: 10.1109/HSI.2017.8005042.

[36] L. Grazi, E. Trigili, G. Proface, F. Giovacchini, S. Crea, and N. Vitiello, “Design and Experimental Evaluation of a Semi-Passive Upper-Limb Exoskeleton for Workers with Motorized Tuning of Assistance,” *IEEE Trans. Neural Syst. Rehabil. Eng.*, vol. 28, no. 10, pp. 2276–2285, 2020, doi: 10.1109/TNSRE.2020.3014408.

[37] B. M. Otten, R. Weidner, and A. Argubi-Wollesen, “Evaluation of a Novel Active Exoskeleton for Tasks at or above Head Level,” *IEEE Robot. Autom. Lett.*, vol. 3, no. 3, pp. 2408–2415, 2018, doi: 10.1109/LRA.2018.2812905.

[38] S. Kim, M. A. Nussbaum, M. I. Mokhlespour Esfahani, M. M. Alemi, S. Alabdulkarim, and E. Rashedi, “Assessing the influence of a passive, upper extremity exoskeletal vest for tasks requiring arm elevation: Part I – ‘Expected’ effects on discomfort, shoulder muscle activity, and work task performance,” *Appl. Ergon.*, vol. 70, no. December 2017, pp. 315–322, 2018, doi: 10.1016/j.apergo.2018.02.025.

[39] A. Moyon, E. Poirson, and J. F. Petiot, “Experimental study of the physical impact of a passive exoskeleton on manual sanding operations,” *Procedia CIRP*, vol. 70, pp. 284–289, 2018, doi: 10.1016/j.procir.2018.04.028.

[40] A. de Vries, M. Murphy, R. Könemann, I. Kingma, and M. de Looze, “The Amount of Support Provided by a Passive Arm Support Exoskeleton in a Range of Elevated Arm Postures,” *IISE Trans. Occup. Ergon. Hum. Factors*, vol. 7, no. 3–4, pp. 311–321, 2019, doi: 10.1080/24725838.2019.1669736.

[41] S. De Bock *et al.*, “Passive Shoulder Exoskeletons: More Effective in the Lab Than in the Field?,” *IEEE Trans. Neural Syst. Rehabil. Eng.*, vol. 29, no. 2016, pp. 173–183, 2021, doi: 10.1109/TNSRE.2020.3041906.

[42] “Fondazione Ergo Publishes Ergonomic Assessment Worksheet Using the MATE Exoskeleton Exoskeleton Report.” https://exoskeletonreport.com/2020/08/fondazione-ergo-publishes-ergonomic-assessment-worksheet-using-the-mate-exoskeleton/ (accessed Apr. 21, 2021).

[43] J. P. Pinho *et al.*, “A comparison between three commercially available exoskeletons in the automotive industry: An electromyographic pilot study,” *Proc. IEEE RAS EMBS Int. Conf. Biomed. Robot. Biomechatronics*, vol. 2020-Novem, pp. 246–251, 2020, doi: 10.1109/BioRob49111.2020.9224362.

[44] N. Jarrassé, “Contributions à l’exploitation d’exosquelettes actifs pour la rééducation neuromotrice,” 2011, Accessed: Apr. 29, 2021. [Online]. Available: https://tel.archives-ouvertes.fr/tel-00641079.

[45] P. Garrec, J. P. Friconneau, Y. Méasson, and Y. Perrot, “ABLE, an innovative transparent exoskeleton for the upper-limb,” *2008 IEEE/RSJ Int. Conf. Intell. Robot. Syst. IROS*, pp. 1483–1488, 2008, doi: 10.1109/IROS.2008.4651012.

[46] R. Singer, C. Maufroy, and U. Schneider, “Automatic support control of an upper body exoskeleton — Method and validation using the Stuttgart Exo-Jacket,” *Wearable Technol.*, vol. 1, pp. 1–13, 2020, doi: 10.1017/wtc.2020.1.

[47] M. Xiloyannis, D. Chiaradia, A. Frisoli, and L. Masia, “Physiological and kinematic effects of a soft exosuit on arm movements,” *J. Neuroeng. Rehabil.*, vol. 16, no. 1, pp. 1–15, 2019, doi: 10.1186/s12984-019-0495-y.

[48] “IUVO - Wearable Technology, Uplifted Life.” https://www.iuvo.company/ (accessed Oct. 08, 2021).

[49] F. Giovacchini, M. Moise, G. Proface, and N. Vitiello, “System for assisting an operator in exerting efforts,” WO2020/217191A1, 2020.

[50] T. Proietti *et al.*, “Sensing and Control of a Multi-Joint Soft Wearable Robot for Upper-Limb Assistance and Rehabilitation,” *IEEE Robot. Autom. Lett.*, vol. 3766, no. c, pp. 1–8, 2021, doi: 10.1109/LRA.2021.3061061.

[51] H. J. Hermens, B. Freriks, C. Disselhorst-Klug, and G. Rau, "Development of recommendations for SEMG sensors and sensor placement procedures," *J. Electromyogr. Kinesiol.*, vol. 10, no. 5, pp. 361–374, Oct. 2000, doi: 10.1016/S1050-6411(00)00027-4.

[52] J. Theurel, K. Desbrosses, T. Roux, and A. Savescu, "Physiological consequences of using an upper limb exoskeleton during manual handling tasks," *Appl. Ergon.*, vol. 67, no. October 2017, pp. 211–217, 2018, doi: 10.1016/j.apergo.2017.10.008.